

# The **Neogene**-Quaternary geodynamic evolution of the Central Calabrian Arc: a case study from the western Catanzaro Trough Basin.

F. Brutto<sup>1</sup>, F. Muto<sup>1</sup>, M.F. Loreto<sup>2</sup>, N. De Paola<sup>3</sup>, V., Tripodi<sup>1</sup>, S. Critelli<sup>1</sup>, L. Facchin<sup>4</sup>

<sup>1</sup> Dipartimento di Biologia, Ecologia e Scienze della Terra (DiBEST)- Università della Calabria, 87036 Arcavacata di Rende (CS), Italy

<sup>2</sup> Istituto di Scienze Marine – Consiglio Nazionale delle Ricerche, U.O.S. Via Gobetti 101, 40129 Bologna, Italy

<sup>3</sup> Department of Earth Sciences, University of Durham, Durham DH1 3LE, UK

<sup>4</sup> Istituto Nazionale di Oceanografia e di Geofisica Sperimentale - OGS, Borgo Grotta Gigante 42/C, 34010 Sgonico (TS), Italy

Corresponding author: [fabrizio.brutto@gmail.com](mailto:fabrizio.brutto@gmail.com) (F.Brutto)

## Abstract

The Catanzaro Trough is a Neogene-Quaternary basin developed in the central Calabrian Arc, between the Serre and the Sila Massifs, and filled by up to 2000 m of continental to marine deposits. It extends from the Sant'Eufemia Basin (SE Tyrrhenian Sea), offshore, to the Catanzaro Basin, onshore. Here, onshore structural data have been integrated with **structural features interpreted using** marine geophysical data to infer the main tectonic processes that have controlled the geodynamic evolution of the western portion of the Catanzaro Trough, since Upper Miocene to present.

The data show a complex tectonostratigraphic architecture of the basin, which is mainly controlled by the activity of NW–SE and NE–SW trending fault systems. In particular, **during late Miocene**, the NW-SE oriented faults system was characterized by left lateral kinematics. The same **structural regime** produces secondary fault systems represented by E-W and NE-SW oriented faults. The ca. E-W lineaments show extensional kinematics, which may have played an important role during the opening of the WNW–ESE paleo-strait; whereas the NE-SW oriented system represents

26 the conjugate faults of the NW-SE oriented structural system, showing a right lateral component of  
27 motion. During the Piacenzian-Lower Pleistocene, structural field and geophysical data show a  
28 switch from left-lateral to right-lateral kinematics of the NW-SE oriented faults, due to a change of  
29 the stress field. This new structural regime influenced the kinematics of the NE-SW faults system,  
30 which registered left lateral movement. Since Middle Pleistocene, the study area experienced an  
31 extensional phase, WNW-ESE oriented, controlled mainly by NE-SW and, subordinately, N-S  
32 oriented normal faults. This type of faulting splits obliquely the western Catanzaro Trough,  
33 producing up-faulted and down-faulted blocks, arranged as graben-type system (i.e. Lamezia Basin).

34 The multidisciplinary approach adopted, allowed us to constrain the structural setting of the  
35 central Calabria segment. The joined onshore with offshore structural data analysis allowed us to  
36 image a more faithful geodynamic evolution of the Calabrian Arc, included in the wider  
37 geodynamic framework of the Mediterranean region

38 Moreover, our results show the close correlation between the NE-SW and N-S normal fault  
39 systems and evidence of deformed Quaternary deposits. These findings are relevant to seismic  
40 hazard understanding in an area which is historically considered at the highest risk of earthquake  
41 and tsunami and where are present important infrastructures and Cities.

42 KEY WORDS: Calabrian Arc, strike-slip faults, normal kinematics, faults reactivation.

43

## 44 1. Introduction and aim of the work

45 Strike-slip fault systems frequently control the opening of sedimentary basins showing a  
46 heterogeneous geometry, due to the development of pull-apart and fault wedge basins at fault bends  
47 and oversteps. These are transtensional basins *sensu stricto* (Ingersoll and Busby, 1996)  
48 characterized by highly geo-structural complexity (Allen et al., 1998; Ingersoll, 2012), due to local  
49 oblique extension with respect to the trends of the main transcurrent faults. Basins formed by

50 transtension are commonly characterized by *en' echelon* arrays of normal faults obliquely oriented  
51 to the boundaries of the deformational zone (Allen et al., 1998; Waldrom, 2005; De Paola et al.,  
52 2006). Transcurrent tectonics **is** also common in obliquely convergent settings where interplate  
53 strain is partitioned into arc-parallel strike-slip zones within the fore-arc, arc or back-arc region  
54 (Fitch, 1972; Beck, 1983; Jarrard 1986; Sylvester, 1988; Diament et al., 1992; Hanus et al., 1996;  
55 Sieh and Natawidjaja, 2000; De Paola et al., 2005; **Cunningham and Mann, 2007**). Moreover, strike-  
56 slip systems, in this geological setting, can rotate and act as elements of accommodation.

57         The Calabrian Arc (Fig.1) is considered one of the most interesting subduction systems due to  
58 the high level of structural complexity. Since the Tortonian time, strike-slip faults play a relevant  
59 role during the evolution of **this** region, favouring southeastward drifting of the arc and its  
60 fragmentation (Ghisetti et al., 1979; Turco et al., 1990; Finetti and De Ben, 1986; Van Dijk et al.  
61 2000). In this complex tectonic setting, an active extensional regime has produced along the  
62 Tyrrhenian side an extensional belt, running for about 370 km of length from the Crati Basin (**CR**)  
63 to the Hyblean Block (Fig.1). **The** extensional fault systems are predominantly organized in graben-  
64 like structures showing trends spanning from NNE-SSW to NNW-SSE (Monaco and Tortorici  
65 2000; Tortorici et al., 2003; Tansi et al., 2007). **This regional fault belt represents the source of**  
66 **several catastrophic earthquakes, indeed, many authors, with different approaches, recognized and**  
67 **analyzed various seismogenic sources (Tortorici et al., 1995; Bordoni and Valensise, 1998; Monaco**  
68 **and Tortorici, 2000; Jacques et al., 2001; Galli and Bosi, 2003; Neri et al., 2004; Galli et al., 2007;**  
69 **Ferranti et al., 2008; Billi et al., 2008; Rovida et al., 2011; Loreto et al., 2013)**

70         The internal structure of sedimentary basins in the central Calabrian Arc is complex with the  
71 presence of both longitudinal extensional faults and transversal strike-slip fault systems. In the  
72 study area (Fig. 1), the western Catanzaro Trough is bounded by large strike-slip fault zones,  
73 crossing the entire emerged Calabrian Arc from the Ionian to the Tyrrhenian Sea (Finetti and De  
74 Ben, 1986; Tansi et al. 2007; Del Ben et al., 2009; Milia et al., 2009).

75            However, the main controlling factors on the origin of transversal strike-slip zones and  
76            extensional faults are not completely understood, and their role in controlling of the geodynamics of  
77            this area is still under debate.

78            The aim of this work is to describe the Neogene –Quaternary evolution of western Catanzaro  
79            Trough, and to discuss the role played by transverse and longitudinal faults during the development  
80            of this area. A multidisciplinary approach, combining onshore/offshore geological and geophysical  
81            data, has been adopted here to assess the complex structural framework of this key sector, which  
82            develops as element of accommodation between northern and southern the Calabrian Arc.

83

## 84            **2. Geological setting**

### 85            *2.1 Geodynamic setting of Calabrian Arc-southern Apennine system*

86            The western Catanzaro Trough represents a Neogene - Quaternary sedimentary basin  
87            belonging to a well-developed *arc-shaped* structure, the Calabrian Arc (Amodio-Morelli et al.,  
88            1976; Tortorici, 1982). The Calabrian Arc is a fragment of Alpine chain connecting the southern  
89            Apennines with the Maghrebide belt. The convergence between the Nubia and Eurasia plates (inset  
90            in Fig. 1) controlled the NW-subduction and the SE-ward roll-back of the Ionian slab that, in turn,  
91            caused rapid SE migration of the Calabrian block (Malinverno and Ryan, 1986; Mantovani et al.,  
92            1990; Dewey et al., 1998; Faccenna et al., 2005). The slab roll-back is accompanied by opposite  
93            rotations along vertical axis at its northern and southern NW-SE oriented edges (Mattei et al.,  
94            2007), the Pollino and Taormina shear zones, respectively (Fig. 1; Ghisetti and Vezzani, 1982; Van  
95            Dijk et al., 2000; Langone et al., 2006; Angi et al., 2010). The E- and SE-ward rapid trench  
96            migration also caused the fragmentation of the Calabrian Arc into structural highs and longitudinal  
97            and transversal sedimentary basins (Ghisetti, 1979; Tansi et al., 2007; Zecchin et al., 2012; Tripodi

98 et al., 2013; Critelli et al., 2013; Muto et al., 2014; Fabbriatore et al., 2014; Longhitano et al., 2014;  
99 Zecchin et al., 2015), including the Catanzaro Trough.

## 100 Figure

101 During Neogene-Quaternary the Calabrian Arc experienced extensional alternated to  
102 contractional or transpressional tectonic phases (Van Dijk et al., 2000; Muto and Perri 2002; Tansi  
103 et al., 2007). In particular during Middle-Upper Pleistocene, the tectonic regime in the Calabria  
104 region passes from transcurrent to extensional regime (Malinverno and Ryan, 1986; Westway,  
105 1993; Van Dijk and Scheepers, 1995; Van Dijk et al., 2000; Minelli and Faccenna, 2010). The  
106 opening of the Tyrrhenian back-arc basin related to the Ionian subduction beneath the Calabrian Arc  
107 is characterized by tensional axes perpendicular to the chain. At the present, according to some  
108 authors, the Ionian slab has partially or completely undergone detachment (Wortel and Spakman,  
109 1992; Guarnieri et al., 2006; Neri et al., 2009). In response to the Ionian slab detachment, the whole  
110 Calabrian Arc undergoes a general tectonic rebound (uplift), at a rate of 0.5–1.2 mm/yr in the last  
111 1–0.7 My, when the propagating tear passes underneath the plate margin segment (Monaco et al.,  
112 1996; Wortel and Spakman, 2000).

113 All these observations suggest that the roll-back in the Tyrrhenian - Calabrian system has  
114 either currently stopped or significantly slowed down (D'Agostino et al., 2004; Serpelloni et al.,  
115 2007, 2010).

## 116 *2.2 Tectono-stratigraphic features of the Catanzaro Trough*

117 The study area is located in the western Catanzaro Trough, along the Tyrrhenian side of  
118 central Calabria, and represents a linkage zone between the northern and southern sectors of the  
119 Calabrian Arc (Fig. 1), which experienced different tectonic phases leading to the development of  
120 both longitudinal and transversal faults systems (Ghisetti, 1979; Monaco and Tortorici, 2000).

121 Longitudinal fault systems are represented by **highly dipping** NE-SW and N-S oriented  
122 normal faults, that are part of the Siculo-Calabrian rift zone (Fig. 2; Monaco et al., 1997; Monaco  
123 and Tortorici, 2000) **and bounding N-S and NE-SW** elongated basins extending along the Calabrian  
124 Arc until eastern Sicily. The several order marine terraces onland-observed along the Tyrrhenian  
125 coast are related with the strong uplift that the Calabrian block **experienced during the Quaternary**  
126 (Westaway, 1993; Mihauchy et al., 1994; Tortorici et al., 2003; Bianca et al., 2011).

127 Transversal fault systems border the northern and southern edges of the Catanzaro Trough  
128 (Fig. 2; Van Dijk et al. 2000; Tansi et al., 2007; Milia et al., 2009). Its northern margin is  
129 represented by a regional NW-SE-trending left-lateral strike-slip faults system. These structural  
130 lineaments consist of three right-stepping *en' echelon* S-dipping major fault segments. The southern  
131 segment is represented by the Lamezia-Catanzaro Fault (Fig. 2; **Monaco and Tortorici, 2000**; Tansi  
132 et al., 2007), recognizable by the evident morphological escarpments with triangular and trapezoidal  
133 facets. The southern margin of the basin is bordered partially by the WNW-ESE oriented, NNE-  
134 dipping Maida –Stalettì Fault Zone (Fig. 2; Ghisetti, 1979; **Monaco and Tortorici, 2000**; Langone et  
135 al., 2006).

136 Figure 2

137 The Catanzaro Trough is filled by Neogene- Quaternary sedimentary succession, (Ferrini and  
138 Testa, 1997; Cianflone and Dominici, 2011; Chiarella et al., 2012; Longhitano et al., 2014). These  
139 deposits unconformably overlie igneous-metamorphic units (Fig. 3, Cavazza and De Celles, 1998).

140 Figure 3

141 The basement rocks are made of Paleozoic **medium to high grade metamorphic rocks** intruded  
142 by plutonic bodies, belonging to the *Calabride Complex (Sila and Castagna Units in Fig. 3;*  
143 *Ogniben, 1969; Amodio-Morelli et al., 1976; Messina et al., 1991a, 1991b, 1994; Critelli et al.,*  
144 *2011)*. These tectonic units are, in turn, tectonically overthrust on the Jurassic to Early Cretaceous  
145 ophiolite-bearing sequences (Bousquet, 1963; Vezzani, 1967; Ogniben, 1973; Amodio-Morelli et

146 al., 1976; Tortorici, 1982; Critelli et al., 2013). These units are referred to the Liguride Complex  
147 (*Metapelitic and Ophiolitic Units* in Fig.3; Ogniben, 1969; Knott, 1987; Liberi et al., 2006), **which**  
148 **together rest tectonically on the *Mesozoic Carbonate Complex* (Fig.3)**

149 The sedimentary succession of the Catanzaro Trough consists of clastic and carbonate strata  
150 (Fig. 4a) of Neogene-Quaternary age.

151 The basal portion of **this** succession is depicted by the Serravallian–Tortonian transgressive  
152 sequence consisting of thinning- and deepening-upward successions. **These units**, assimilated to the  
153 **Serravallian- Tortonian deposits** of the Amantea Basin (Colella, 1995; Muto and Perri, 2002), **rarely**  
154 **outcrop along the margins of the western Catanzaro Trough.**

155 Then the Messinian evaporitic succession (*Calcare di Base and Gypsum Fms*; Fig. 4a) starts  
156 **to be laid down, reaching ca. 100 m of thickness** (Cavazza and Ingersoll., 2005; Roveri et al., 2008;  
157 Barone et al., 2008; Govers et a., 2009; Manzi et al., 2010; Zecchin et al., 2013a, 2013b; Brutto et  
158 al., 2015).

159 The end of Messinian Salinity Crisis is marked by a late Messinian to Lower Pliocene  
160 continental succession, up to 150 m-thick (*late Messinian to early Pliocene Conglomerate*; Fig. 4b).  
161 These deposits are coeval to the Carvane Fm (Roda, 1964; Barone et al., 2008; Zecchin et al.,  
162 2013b).

163 The 300 m-thick Pliocene Siltstones and marls (Fig. 4b) outcrop widely in the study area and  
164 show an affinity with the Trubi formation cropping out along the peri-Ionian Neogene basins  
165 (Cavazza and DeCelles, 2004; Tripodi et al., 2013; Zecchin et al., 2013a). These deposits pass  
166 upward to a ca. 100 m-thick succession correlated to the Monte Narbone Fm (Piacenzian) (Fig. 4c;  
167 Di Stefano and Lentini, 1995; Cavazza et al., 1997; Bonardi et al., 2001).

168 Figure 4

169 The early Pleistocene unconformity (EPSU in Zecchin et al., 2012, 2015) marks the opening  
170 of the Catanzaro fault-bounded paleo-strait (sensu Longhitano et al., 2014), characterized by ca. 100

171 m of mixed, silici-bioclastic, sands and sandstones (Figs. 4d and e; Chiarella, 2011; Chiarella et al.,  
172 2012; Longhitano et al., 2012a, 2014).

173 The Middle -Upper Pleistocene generally made of siliciclastic sands and coarse sandstones  
174 with poor fossiliferous content which rest directly on Lower Pleistocene deposits (Figs. 4e and e')  
175 and on the crystalline-metamorphic substrate constituting the margins of the basin. The western part  
176 of the Catanzaro Trough is dominated by outcrops of Late Quaternary 60 m-thick conglomerate and  
177 sand deposits (Alluvial Fans; see geological map in Fig. 3).

178

### 179 **3. Materials and methods**

180 The Catanzaro Trough is characterized by a complex geo-structural history with one of the  
181 highest seismic moment release of the whole Italy (Gasparini et al., 1982; Westway, 1993; Calò et  
182 al., 2012). To improve knowledge of the structural setting of this region, we adopted a multi-  
183 disciplinary approach by collecting and analysing new geological and structural data, which have  
184 been integrated with onshore and offshore seismic reflection profiles and high-resolution morpho-  
185 bathymetry data.

#### 186 *3.1 On-land structural data*

187 Fieldwork has been mainly performed in the western margin of the Catanzaro Trough. Field  
188 observations and structural data, such as fault orientations and kinematics, have been collected for  
189 brittle features, and have been used to infer their evolution in the study area. More than 500  
190 structural measurements have been collected at 35 stations (Fig.7), and have been analysed and  
191 processed using the DAISY software (Salvini, 2002).

192 In particular, the statistical distribution of faults and their kinematics has been analysed by  
193 contouring of fault planes and associated slickensides. Stress inversion techniques relying on  
194 rotational axes (rotaxes), which correspond to the  $\sigma_2$  axis of a conjugate pair of andersonian faults,



195 have been performed on sets of fault planes and kinematic indicators to discriminate between the  
196 different deformation events, using the Daisy software (Wise and Vincent, 1965; Salvini & Vittori,  
197 1982; Mattei, et al., 1999).

198 Figure 5

### 199 3.2 Multichannel seismic profiles and wells by ViDEPI project

200 In order to bridge the gap of lack of structural data along the Tyrrhenian coastal areas, four  
201 multichannel seismic profiles (located both onshore and offshore) and two wells (Marta and Marisa;  
202 Figs. 5 and 6) were analysed. These data were acquired within the Sant'Eufemia Gulf and onshore  
203 Lamezia Plain by Eni s.p.a. at the beginning of the 80', and made available in the frame of the  
204 ViDEPI project (Fig. 5). In spite of their low quality, the ViDEPI seismic profiles have provided,  
205 together with Marta and Marisa wells (Fig. 6), some constraints in the seismo-stratigraphy of the  
206 Catanzaro Trough basin.

207 Figure 6

### 208 3.3 High resolution morpho-bathymetry

209 High resolution morpho-bathymetric map (Fig. 5) acquired during the R/V OGS-Explora  
210 campaign in summer of 2010, in the frame of ISTEGE project (Loreto et al., 2012), has been made  
211 available by ISMAR - CNR U.O.S. of Bologna. The data were performed with a grid cell size of 20  
212 x 20 m, obtained by using two hull mounted Multibeam echosounders: the Reson Seabat 8111  
213 (nominal frequencies of work: 100 kHz), and the Reson Seabat 8150 (nominal frequencies of work:  
214 12 kHz). More details about acquisition and processing of multibeam data can be found in Loreto et  
215 al. (2012).

### 216 3.4 Offshore Multichannel seismic data

217 Multichannel seismic (MCS) profiles have been acquired in the northeastern portion of the  
218 Sant'Eufemia Gulf (Fig. 5), in the frame of ISTEGE project (Loreto et al., 2012).

219 Within the gulf, about 300 km of middle resolution MCS profiles were collected by using  
220 1500 m-long streamer cable, 120-channel array with 12.5 m trace interval. The energy source  
221 consisted of two GI-guns with a total volume of 8-liters, shooting every 25 m, with a resulting  
222 seismic coverage of 30 for each investigated depth point (Loreto et al., 2012; 2013 for further  
223 details). These data allowed the investigation of the entire Pliocene-Pleistocene sedimentary  
224 sequence and the upper part of the Messinian rocks. In particular, five seismic MCS profiles (light  
225 green lines in Fig. 5), were interpreted to study the offshore tectonics of the western Catanzaro  
226 Trough, although only two MCS lines have been showed in this work.

227 Management and interpretation of seismic profiles were performed using the *Kingdom*  
228 software (IHS Gobal Inc.).

### 229 3.5. 1-kJoul Minisparker profiles

230 Eight NNW-SSE striking single-channel seismic profiles (1-kJ Sparker), acquired aboard the  
231 R/V Bannock (Trincardi et al., 1987), were integrated with ISTEGE data, even though here, we  
232 displayed only Vp9 Sparker profile. Sparker profiles (see location in Fig. 7), acquired with a broad  
233 band (100 - 2000 Hz), achieved better acoustic penetration, up to 1 sec in TWT. They were fired  
234 every 2s, recorded with a 2-s sweep and a band-pass filter of 100 - 600 Hz (Trincardi et al., 1987).

235

## 236 4. Results

### 237 4.1 Structural data

238 Structural data analysis based on the statistical distribution of fault orientation and associated  
239 kinematic indicators (DAISY software; Salvini, 2002), allowed us to identify several fault sets,  
240 underlining a prevalence of normal kinematics (Fig. 7). The great variability of faults (Fig. 7),

241 affecting the Neogene-Quaternary basin infill, provides clues on chronological evolution of the  
242 area; along the NW-SE and NE-SW major faults, these deposits are brought into contact with Paleo-  
243 Mesozoic crystalline-metamorphic and sedimentary rocks of substrate.

244 Figure 7

245 Notwithstanding the E-W long-shaped basin, a great number of N-S and NE-SW normal  
246 faults have been measured (Fig.7).

247 Minor NW-striking, strike-slip faults affect the basin (Fig 8a). Evidence of the kinematics of  
248 these faults system is highlighted locally when these come into contact with the underlying  
249 basement rocks, allowing us to define the main kinematics features of these fault planes (Fig. 8b).

250 Figure 8

251 Fault planes, showing more than one set of **striations**, and cross-cutting relationships between  
252 two or more fault systems are used to reconstruct the evolutionary stages characterizing the western  
253 Catanzaro Trough. **We identified three tectonic phases:**

254 **1)** In the Upper Miocene-Pliocene basin infill, three main fault systems have been recognized  
255 and documented: **a)** a NW-SE fault system, which shows sub-vertical fault planes, equally dipping  
256 both towards SW and towards NE (Fig. 9a). Slickensides document a relative abundance of left  
257 lateral strike-slip faults (Fig. 9a'), although normal component of motion have been also measured;  
258 **b)** The faults system striking from WNW-ESE to WSW-ENE is characterized by dip-slip striations  
259 with pitches ranging from 60° to 90° (Figs. 9b and b'). These structural lineaments **display sub-**  
260 **vertical fault planes and represent, together with NW-SE strike-slip faults,** the northern and  
261 southern morpho-structural bounds of the Catanzaro Trough. **In these tectonic setting, we observed**  
262 **locally, c) secondary NE-SW oriented faults, displaying, in some cases, strike-slip with reverse**  
263 **component of motion (Figs. 9c and c').**

264 Figure 9

265 2) Three main fault systems have been recognized in the Piacenzian - Lower Pleistocene  
266 deposits: a) WNW-ESE to ENE-WNW reverse faults, showing both right and left- lateral  
267 component of motion, commonly ca. S dipping (Fig. 10a); and b) NE-SW left-lateral structures,  
268 which show slickensides having pitches ranging from 30° to 50°, with sub-vertical fault planes  
269 (Figs. 10b and b'). At the mesoscale these faults have been observed widely within the central and  
270 eastern portion of the area, influencing locally a dipping change of the Lower Pleistocene mixed  
271 strata. c) Minor NW-striking right lateral strike-slip faults have been observed in the area (Fig. 10c),  
272 usually superimposed the left lateral striaes on the same fault planes (see above Fig. 9a). This  
273 suggests an inversion of transcurrent movement.

274 Figure 10

275 3) Within the southwestern side of the study area, a number of NE-SW and N-S faults clearly  
276 dislocate the Middle Pleistocene terraced deposits, showing dip-slip movements with rarely strike-  
277 slip component of motion (Fig. 11).

278 Although the structural data show a wide range of fault orientations and kinematics, the NE-  
279 SW and N-S oriented normal faults represent the most abundant structures in the study area. These  
280 faults correspond with tectonic structures affecting the Quaternary sediments of the basin infill and,  
281 in some case, also crystalline bedrock (Figs. 11a and b). At the mesoscale, these structures show a  
282 sub-vertical fault planes with orientation spanning from N20 (200) to N60 (240), equally dipping  
283 both towards SE/E and towards NW/W (Fig. 11c). The central and eastern border of the basin is  
284 characterized by a series of NE-SW oriented structural lineaments strongly controlling the drainage  
285 pattern (see geological map in Fig. 3).

286 Figure 11

287 4.2. Onshore seismic data

288 **Figure 12** images the W-E oriented CZ-329-78 MCS ViDEPI profile. This profile images the  
289 Miocene unit, which top corresponds to an high amplitude and very continue seismic reflector,  
290 covered by a **better** stratified, even if poorly continue, sedimentary unit corresponding to Pliocene-  
291 Quaternary deposits. **The boundaries between different units are constrained by the seismo-**  
292 **stratigraphic character (Dumas et al., 1987) of the lithologies described in the Marta and Marisa**  
293 **wells and the time to depth conversion assuming, for the Pliocene-Quaternary sediments, a constant**  
294 **seismic velocity of 2200 m/s (Pepe et al., 2010).** These units are characterized by numerous  
295 discontinuities and fault-controlled dislocations, mainly with normal and, sporadically, **reverse**  
296 kinematics. Amongst shot points **(SP)** 160 – 190, thickness increase of Pliocene-Quaternary  
297 sediments and the evident dislocation of the Miocene top reveal the activity of a W-dipping normal  
298 fault (Fig. 12). This newly identified San Pietro Lametino normal Fault is NE-SW oriented, as  
299 derived by unpublished ViDEPI profiles and Vigor well data.

300 Figure 12

#### 301 4.3 Offshore seismic data

302 In the offshore, we have interpreted two parallel ViDEPI seismic profiles, ER-77-502 and ER-  
303 77-3028, NW-SE oriented (**Fig. 13**). The well stratified Pliocene-Quaternary sequences lie on the  
304 top of the Miocene, which is represented by a highly continuous horizon with high amplitude due to  
305 the strong acoustic contrast between conglomerates (Messinian) and marls (Pliocene). **In the**  
306 **northeastern part of the ER-77-502** the Upper Miocene-Pliocene sediments are highly deformed (SP  
307 100 - 190) forming a gentle anticline confined within the Lower Pliocene (**Structural High**), **this**  
308 **deformation becomes less pronounced in the ER-77-3028**. Whereas in the southeastern part only  
309 **gently folded units** are detectable **in both profiles** (Fig. 13; *Transpressional/ compressional faults*).  
310 **The deformations imply** a NNE-SSW oriented compressional system.

311 ER-77-502 and ER-77-3028 ViDEPI MCS profiles show amongst SP 178-200 and 20-40,  
312 respectively, a normal fault that controls the deepening of the basin towards the onshore **and border**

313 the Structural High (Fig. 13). This structure is result of growth of fold anticline related to the  
314 propagation of thrust fault and involving the Pliocene deposits. Considering the orientation and  
315 location of these two profiles and the previous work (Loreto et al., 2013), we suggest that the  
316 recognized faults are part of the NE-trending Sant'Eufemia normal fault, which locally outcrop at  
317 the seafloor (see Figs. 5 and 10 in Loreto et al., 2013). Further, in the ER-77-3028 profile, this fault  
318 reaches 2.4 s (TWT, two-way traveltime) of depth, displacing ill-defined horizons, here named  
319 Deep Horizons. We estimate that the Deep Horizons are offset more than 0,6 s (TWT) (Fig. 13).

320 Figure 13

321 In the central part of the gulf, two NE-SW-striking multichannel seismic profiles (Fig.14)  
322 show a SW-facing, E-W trending Master Fault and its antithetic lineaments, deforming differently  
323 from top to bottom the entire Neogene-Quaternary sedimentary basin. The deformation, confined  
324 between Upper Miocene and Lower Pleistocene, produces Pliocene deposits thickening in the  
325 hangingwall respect to the footwall across the Master Fault (Fig.14). Although this deformation  
326 changes slightly moving from one profile to the other, the fault dislocation measured at the top of  
327 the Miocene changes substantially from ca. 0,3 s (TWT), in the GSE10\_05 profile, to ca. 0,1 s  
328 (TWT) in the GSE10\_04 profile. Sediment deformation increases up-ward, indeed the dislocation is  
329 replaced by folding with associated anticline growth. This deformation is confined amongst Upper  
330 Pliocene and Lower Pleistocene layers (ranging from about 0,8 and 1,6 s-(TWT) for both MCS  
331 profiles). Therefore an initially extensional/ transtensional mode of fault (Williams et al., 1989) is  
332 replaced by an apparent reversal or transpressional movement.

333 Figure 14

334 Three small ridges NE-SW oriented have been identified in the high-resolution morpho-  
335 bathymetry map (black fold axes in Fig.15a) and in the Vp9 Sparker seismic line (Fig. 15b) located  
336 in the center of the Sant'Eufemia Gulf.

337 According to our interpretation these structures can be kinematically associated to the right  
338 lateral with reverse component of movement of Master Faults (inset a' in fig. 15) which, during the  
339 Upper Pliocene-Lower Pleistocene time, replacing the previous normal kinematics.

340 Vp9 Sparker seismic profile (Fig.15b), although not perpendicular to the ridges, images the  
341 sediments of Quaternary succession deformed in sequence of folds placed in the hangingwall of the  
342 Master Fault. The Sparker line shows a more recent *compressional deformation* (Fig. 15b) with  
343 similar orientation to the deformation observed in the MCS ViDEPI profiles (Structural High, Fig.  
344 13). The Vp9 Sparker ridges, in turn, are newly displaced by a series of high angle NE-trending  
345 faults that record an extensional event (Fig. 15b). The orientation of these faults was defined  
346 examining two crossing seismic profiles (Vp9 and GSE10\_08, Fig 15a for their location).

347 Figure 15

348

## 349 5. Discussion

350 The aim of this work is to define the Neogene-Quaternary evolution of the western Catanzaro  
351 Trough, and the role of transverse and longitudinal faults in controlling the evolution of the northern  
352 and southern sectors of the Calabrian Arc.

353 Many authors highlighted how the continental collision in northern Calabria and central-  
354 western Sicily caused strong lithosphere deformation in correspondence to a series of tear faults  
355 (Fig. 16). After the analysis of geological data and the integration with offshore geophysical data,  
356 Guarnieri (2006) placed one of these tear faults within the central Calabrian Arc showing a N120  
357 trending, which provoke the segmentation of this forearc/ backarc system (Fig. 16).

358 More recently Chiarabba et al., (2008) and Neri et al., (2009), by means of seismic dataset and  
359 tomographic inversion, consider that the slab is detached beneath northeastern Sicily and northern  
360 Calabria, whereas appears undetached beneath the Messina straits and central Calabria. This leads

361 the authors to suggest that the change between detached/undetached slab occurred within the  
362 Catanzaro Trough, producing a tear fault that acts as releasing tectonic element (Fig. 16).

363 Figure 16

364 Hence, the study area is placed in a key sector to understand the evolution of whole Calabrian  
365 Arc. Combining and analysing onshore and offshore datasets, including structural (more than 500  
366 fault planes measurements) and geophysical data (multibeam data, multichannel and Sparker  
367 profiles), we were able to define the different tectonic phases controlling the opening and evolution  
368 of the Catanzaro Trough since the Late Miocene.

369 The data collected and their interpretation suggest that the structural complexity and evolution  
370 of the Calabrian Arc are due to multiple reactivation events of pre-existing faults, some of which  
371 are in fact polyphase structures. A heterogeneous dispersion of rotaxes demonstrates this hypothesis  
372 (Salvini et al., 1982). Indeed, structural data show a scattered distribution of rotaxes (Fig. 17),  
373 although two main clusters of sub-horizontal and sub-vertical rotaxes can be identified. The sub-  
374 horizontal rotaxes ( $\sigma_2$ ) of normal faults dominate (almost 300 measurements) and are concentrated  
375 around the N30 and N70 directions (Fig. 17). These trends are consistent with N–S and NE–SW  
376 oriented normal fault systems, displaying a ca. NW-SE oriented extensional direction ( $\sigma_3$ ). The sub-  
377 horizontal rotaxes ( $\sigma_2$ ) obtained for reverse faults (Fig. 17) show a greater concentration around the  
378 N45 direction; whereas  $\sigma_1$  is oriented along the NW-SE direction. Sub-vertical clusters of rotaxes  
379 ( $\sigma_2$ ) are obtained for strike-slip faults, they correspond to the left lateral and the right lateral faults  
380 which show a greater scattering of the data distribution (Fig.17) suggesting, here too, faults  
381 reactivation events during the tectonic evolution of the area.

382 Fig. 17

### 383 *5.1. Tectonic events of the western Catanzaro Trough*

384 Three main tectonic events have been recognized based on the ages of the deposits affected by  
385 repeated faulting (Fig. 18).



386 The earliest tectonic phase (Figs. 18a, b, c) is restricted to the Upper Miocene-Lower  
387 Pliocene, and it is well recognized within the Messinian deposits (Figs. 9 and 13), in both onshore  
388 and offshore datasets from the western Catanzaro Trough. Three main fault systems associated to  
389 this tectonic phase have been identified and described onshore: 1- the ca. NW-SE oriented sinistral  
390 strike- slip faults parallel to the Lamezia-Catanzaro Fault (Figs. 9, 18a, sensu Tansi et al., 2007); 2-  
391 the WNW-ESE and the WSW-ENE oriented extensional faults (Figs. 9b), bounding clearly the  
392 northern and southern margins of the Catanzaro Trough; and finally 3 - the NE-SW oriented right-  
393 lateral fault systems (Fig. 9c). Combining these three fault systems, affecting only the Upper  
394 Miocene- Pliocene deposits, an acceptable stress field emerges consistent with an E-W-trending  
395 sub-horizontal  $\sigma_1$  stress axis (Compressional: P-axis; Fig. 18a).

396 The ER-77-502 and ER-77-3028 seismic profiles on the Tyrrhenian offshore display NE-SW-  
397 oriented transpressional faults, arranged as thrust ramps (Fig. 13). The structures observed on both  
398 profiles are compatible with E-W-oriented P-axis, consistent with that inferred from the onshore  
399 datasets. In the center of Sant'Eufemia Gulf the SW-facing, the WNW-trending Master Fault (Figs.  
400 14 and 18b) was active at least until the Piacenzian time as a normal fault. The large offset (ca. 300  
401 ms TWT) rapidly disappears eastward next to the NE-trending ridge, in relation to the activity of  
402 reverse/transpressional faults, associated with the post-Serravallian ESE-ward drifting of the  
403 Calabrian Arc (see also Van Dijk et al., 2000; Muto and Perri 2002; Tansi et al., 2007; Tripodi et  
404 al., 2013).

405 During the Upper Miocene-Pliocene time, the NW-SE faults system assumes, hence, the role  
406 of crustal shear zone which divides the Arc into segments of 'tectonostratigraphic terranes' (Van  
407 Dijk et al., 2000). In this model the extensional WNW-ESE faults accommodate also the  
408 transcurrent movement, and produce a significant increase of the basin-area. This normal faults  
409 could act as margin of a transtensional zone (e.g western Catanzaro Trough), such as occurred in the  
410 Triassic-Jurassic basins in the High Atlas of Morocco (Beauchamp, 1999). According to Allen et al.

411 (1998), in many cases, the deformation zone can be accommodated by the rotation of the oblique  
412 fault blocks within the basin; even though in this study the rotational axes have not been quantified.

413 A second tectonic phase (Figs. 18d, e, f) is inferred from onshore observations with **WNW-**  
414 **ESE trending** reverse/transpressional, NE-SW trending left-lateral faults and **minor NW-SE**  
415 **oriented right lateral faults**, confined below the Middle Pleistocene deposits (Figs. 10a, b and c).  
416 Similar evidences are found in the offshore dataset, where the Lower Pleistocene sediments  
417 **bounded** by the **E-W-trending** Master Fault locally show positive tectonic inversion (Figs. 14 and  
418 18e). Thus, the stratigraphic sequence of sediments in the hangingwall of the Master Fault evolves  
419 from an extensional synrift one, in the Miocene- Pliocene, to a right lateral transpressive one during  
420 the Piacenzian- Lower Pleistocene (Figs.14 and 15). Structural and geophysical data confirm the  
421 presence of an oblique compressional event, consistent with a stress field where the maximum  
422 principal stress axis ( $\sigma_1$ ) shows the sub-horizontal NNW-SSE orientation (Fig. 18d). **The change in**  
423 **the kinematics (e.g. from left to right lateral motion of NW-SE strike-slip faults) of the major faults**  
424 **is simultaneous to the onset of flexural down-bending and detachment of the Ionian subducted slab**  
425 **which causes the cessation of vertical axis rotation as also suggested by several authors (Westaway**  
426 **et al., 1993; Van Dijk and Scheepers 1995; Mattei et al., 2007; Neri et al., 2009; Maffione et al.,**  
427 **2013).**

428 Figure 18

429 A third tectonic phase, acting during the Middle – Upper Pleistocene is inferred from NE–SW  
430 and N–S normal faults systems observed in the field at the mesoscale (Figs. 18g, h, i). This event is  
431 also recorded by the widespread Middle–Upper **Pleistocene** marine terraces, observed along the  
432 Tyrrhenian coastline (Fig.13; Monaco and Tortorici 2000; Cucci and Tertulliani 2010; Bianca et al.,  
433 2011). **These are produced by** the interaction between Quaternary sea-level change cycles **and long-**  
434 **term tectonic uplift driven by NE–SW and WNW–ESE striking normal faults** (e.g. Sant’Eufemia,  
435 Vibo Valentia and San Pietro Lametino Faults) imaged by ViDEPI seismic lines located both

436 offshore and onshore in the western Catanzaro Trough (Figs. 12 and 13). The inferred third tectonic  
437 phase is consistent with a WNW-ESE oriented extension (Fig. 18g) **as consequence of the complete**  
438 **or partial detachment of the Ionian subducted slab (Westaway, 1993; Wortel and Spackman, 2000;**  
439 **Tortorici et al., 2003; Goes et al., 2004, Neri et al., 2012).** These lineaments often offset the late  
440 **Quaternary deposits and are considered to be seismogenic source (Loreto et al., 2013).**

441 During this last tectonic phase, some NE-SW elongated basins were formed within the  
442 Catanzaro Trough, including the *Lamezia Basin* (Fig. 19a). The Lamezia Basin is bounded both to  
443 the north and to the south by regional WNW-ESE trending oblique and strike-slip fault systems,  
444 and laterally by NE-trending normal faults (Fig. 19a).

445 The northern termination of the basin is clearly identifiable with the LCF system, whilst the  
446 southern one is more uncertain. Here, a structural high, the Capo Vaticano promontory, is present  
447 and is bordered to the south by the Coccorino and Nicotera Faults (CF&NF) system (Fig. 19a).

448 The NE-trending Vibo Valentia and San Pietro Lametino Faults control the evolution of the  
449 Lamezia Basin together with the Sant'Eufemia Fault. This basin arranged as a graben-like system is  
450 similar to other graben and semi-graben systems, which are widespread in the Calabrian Arc, such  
451 as the Crati graben, the Mesima graben, and the Gioia Tauro plain (Monaco and Tortorici, 2000).

452 The eastern basin edge **is bounded** by the newly identified W-dipping San Pietro Lametino  
453 Fault (SPLF; Fig. 19a), which could represent the northern propagation of the Vibo Valentia  
454 structural system, organized as a left-stepping en'echelon segment (overstepping lineaments;  
455 Peacock et al., 2000). In this way two segments can join to form a single and much longer fault  
456 (Fig. 19a; Peacock et al., 2000; Kim et al., 2004; Fossen, 2010). The asymmetric displacement  
457 between these two faults produces a folded overlap zone, namely a relay ramp (Peacock et al., 2000,  
458 Fossen, 2010) connecting two overstepping lineaments, which acts as a transfer zone. The presence  
459 of small cracks or secondary faults (*Overstepping Fault* - OF - in Fig. 19a, b, and c) across the relay  
460 ramp may suggest that the bounding faults could be connected at depth (Peacock and Parfitt 2002),

461 even though we have no field evidence, this structure has been inferred by morphological  
462 consideration.

463 Figure 19

464 On the western edge, the Sant'Eufemia Fault (SEF) shows a normal kinematics at least since  
465 the Pleistocene time. Evidence of fault planes, with same orientation and kinematics, have been  
466 recognized even within the onshore area. This suggests that the Sant'Eufemia Fault, extending  
467 through the whole Sant'Eufemia Gulf, could also continue on-land reaching the morphological  
468 northern edge of the Catanzaro Trough and increasing the 25 km fault length, previously proposed  
469 by Loreto et al. (2013), to more than 30 km.

470 Based on these new onshore and offshore data, the Sant'Eufemia Fault together with the other  
471 NE-SW/N-S oriented fault systems assume a much more important role in the frame of the late  
472 Quaternary tectonics. This is in agreement with the WNW-ESE extensional regime obtained by the  
473 crustal focal mechanisms, computed for the study area by using waveform inversion methods (Li et  
474 al., 2007; D'Amico et al., 2010, 2011; Presti et al., 2013).

475

## 476 6. Conclusion

477 The Calabrian Arc is considered to be at an intermediate evolutionary stage between the still  
478 active Aegean subduction system and the mature - inactive Gibraltar Arc subduction system (Mattei  
479 et al., 2007). The integration of geological and geophysical data, acquired along the SE Tyrrhenian  
480 Sea facing the Central Calabrian Arc, allowed us to recognize at least three tectonic stages (see  
481 Fig.18). The first two are characterized by the high rate of rotation during the Late Pliocene-Lower  
482 Pleistocene. Initially, this tectonic setting favoured the development of a sub- horizontal E-W-  
483 oriented compressive P-axis. Later, during Lower Pleistocene, a change of this stress field is  
484 inferred by the ca. NNE-SSW P-axis. Since the Middle Pleistocene, a new tectonic stage

485 characterized the western Catanzaro Trough, which highlights vertical P-axis and WNW-ESE  
486 oriented T-axis.

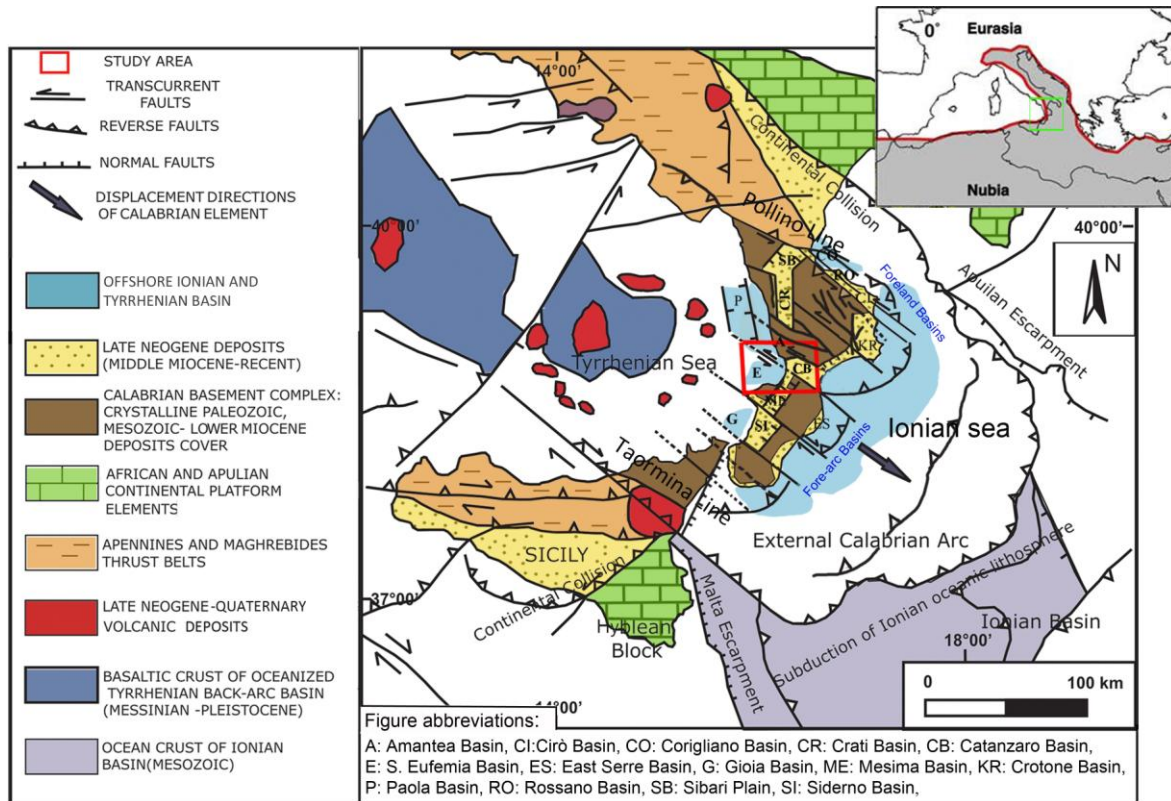
487 Finally, the NW-SE oriented faults and their associated secondary faults are responsible for  
488 opening of a E-W palaeo-strait that connected the Tyrrhenian area to the Ionian Sea during  
489 multiphase tectonics until early Pleistocene. The NE-SW and N-S fault systems bound and control  
490 the late Quaternary sub-basins, arranged as graben system (i.e. Lamezia Basin) in response to one of  
491 the last extensional stages of Tyrrhenian Sea opening.

492 In this scenario, the Catanzaro Trough is placed amongst two blocks: the northern and  
493 southern Calabrian Arc, which represent two different geologic sectors, evolving as two different  
494 geodynamic elements. Subduction slab behaviour and oblique continental collision further  
495 influenced and marked these differences, making the Catanzaro Trough as one of the most  
496 important place to understand the evolution of the entire Mediterranean region.

497 The data collected and presented in this contribution provides new insights and details about  
498 this area, providing valuable structural data even for a future assessment of the seismogenic  
499 potential of an area historically considered with the highest earthquake and tsunami risk throughout  
500 Italy.

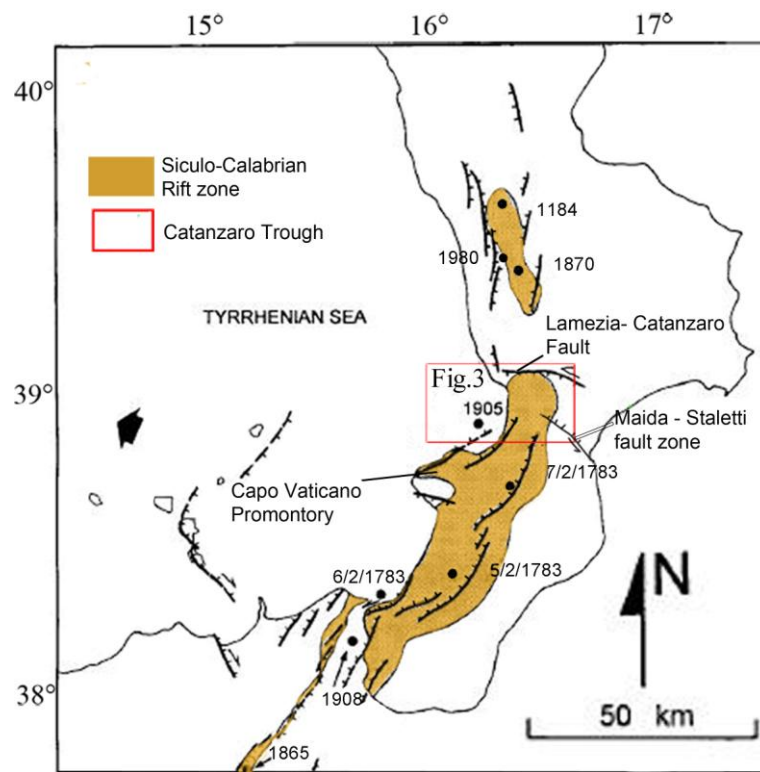
501

## 502 **7. Figures and figure captions**



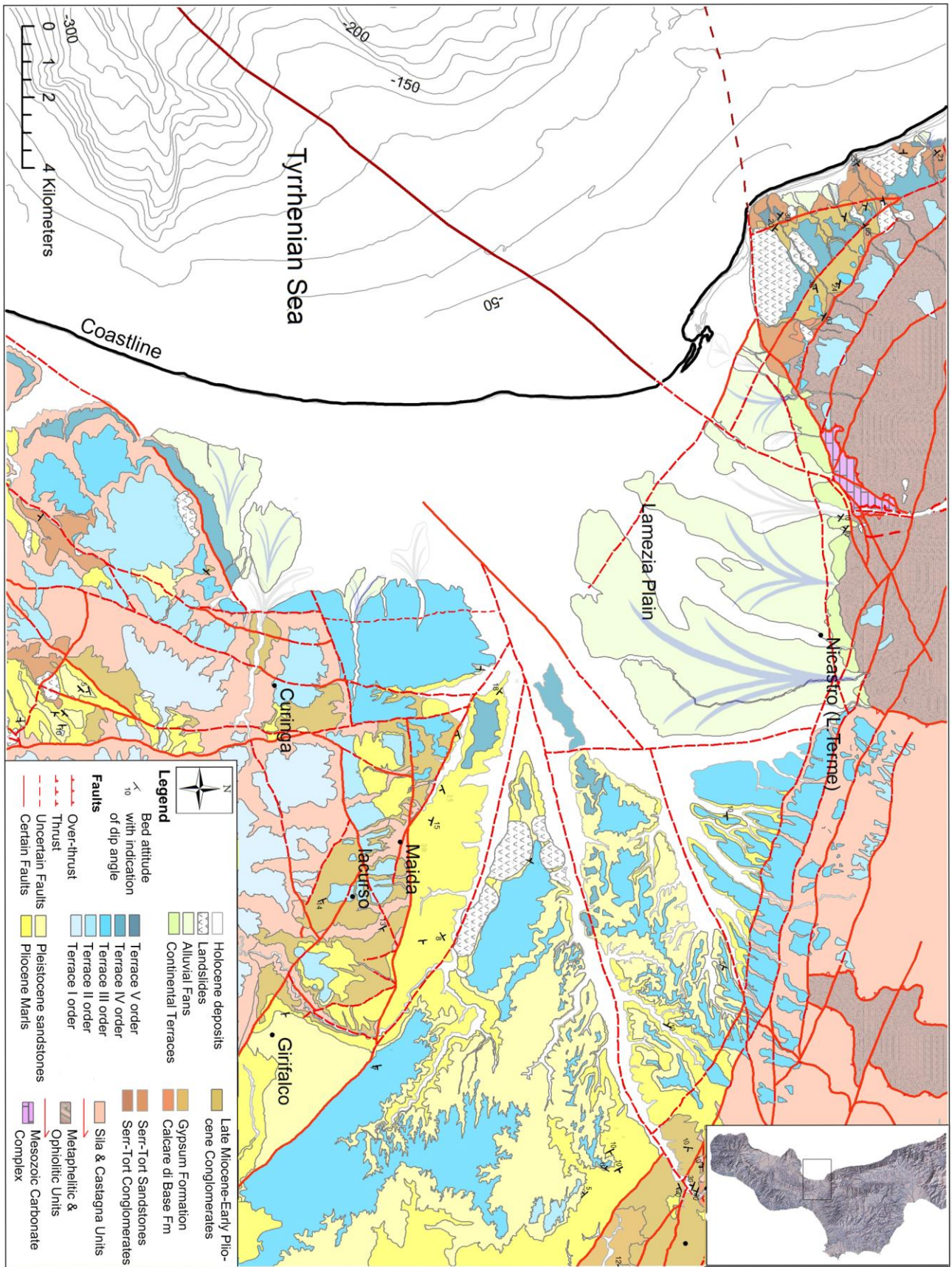
503  
504  
505  
506

Figure 1: The geological framework of the Central Mediterranean region (modified by Van Dijk et al., 2000 and reference therein).



507  
508  
509

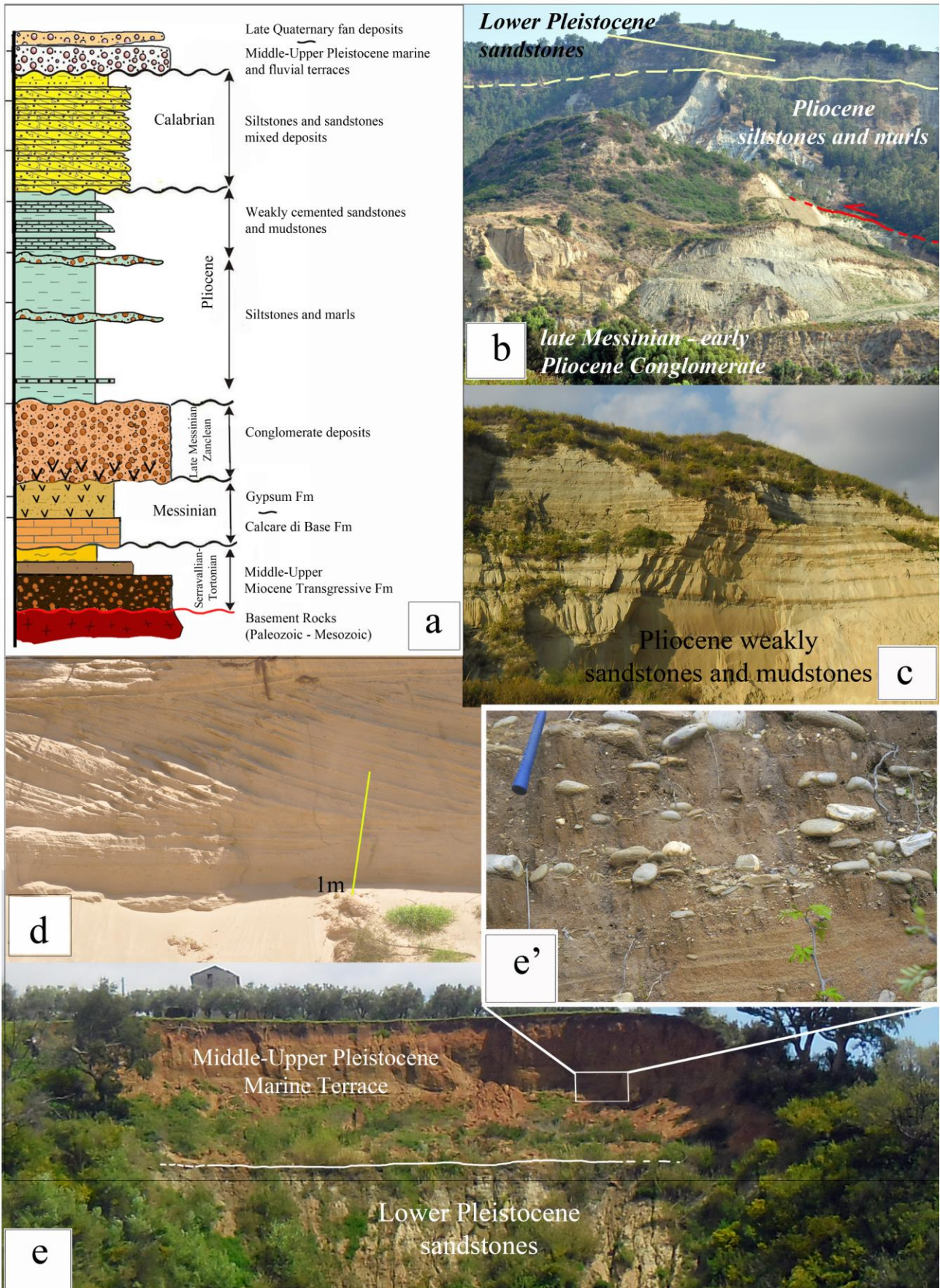
Figure 2: Historical earthquakes and faults along the Siculo-Calabrian Rift zone (modified from Monaco and Tortorici, 2000).



510

511

Figure 3: Geological map of the study area.



512

513

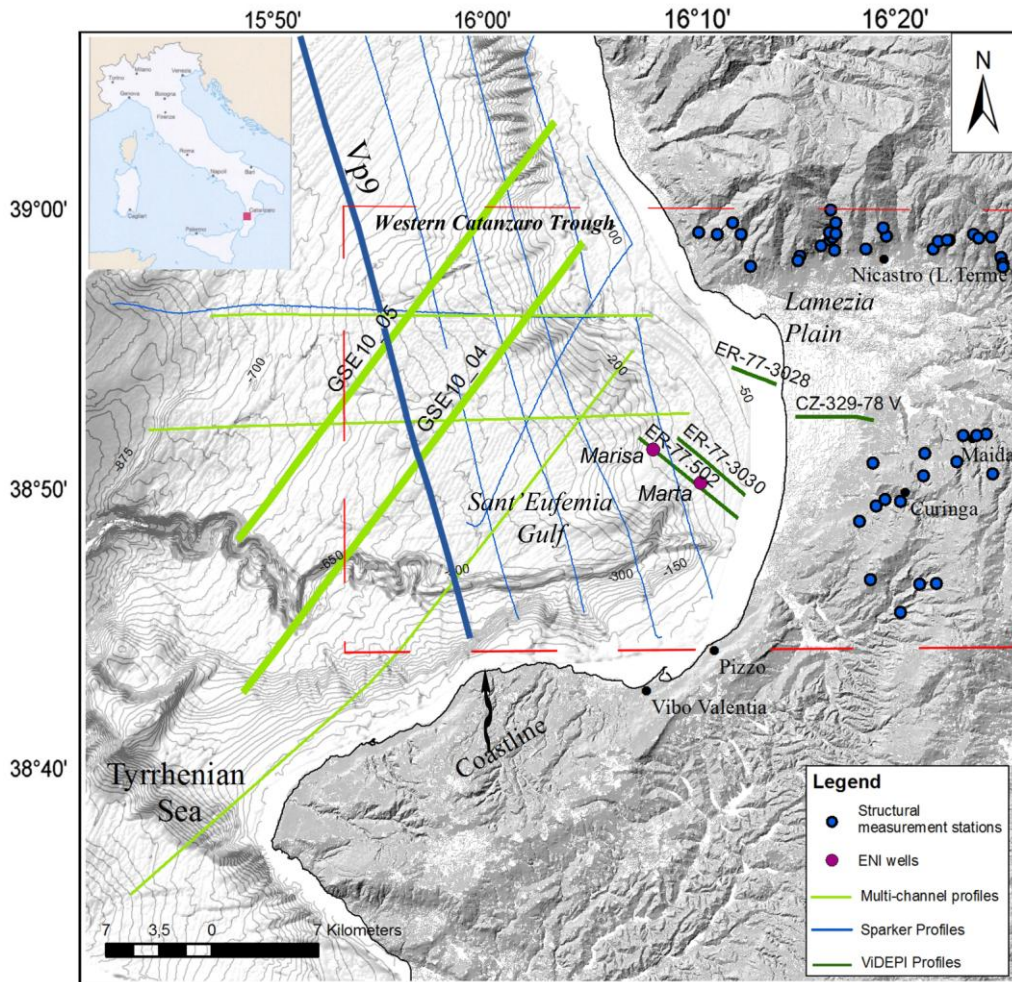
514

Figure 4: a) General stratigraphy of the study area (modified from Chiarella et al., 2011); b) Messinian to Lower Pleistocene units outcropping in the southeastern portion of the area, showing tectonic contact between Conglomerate



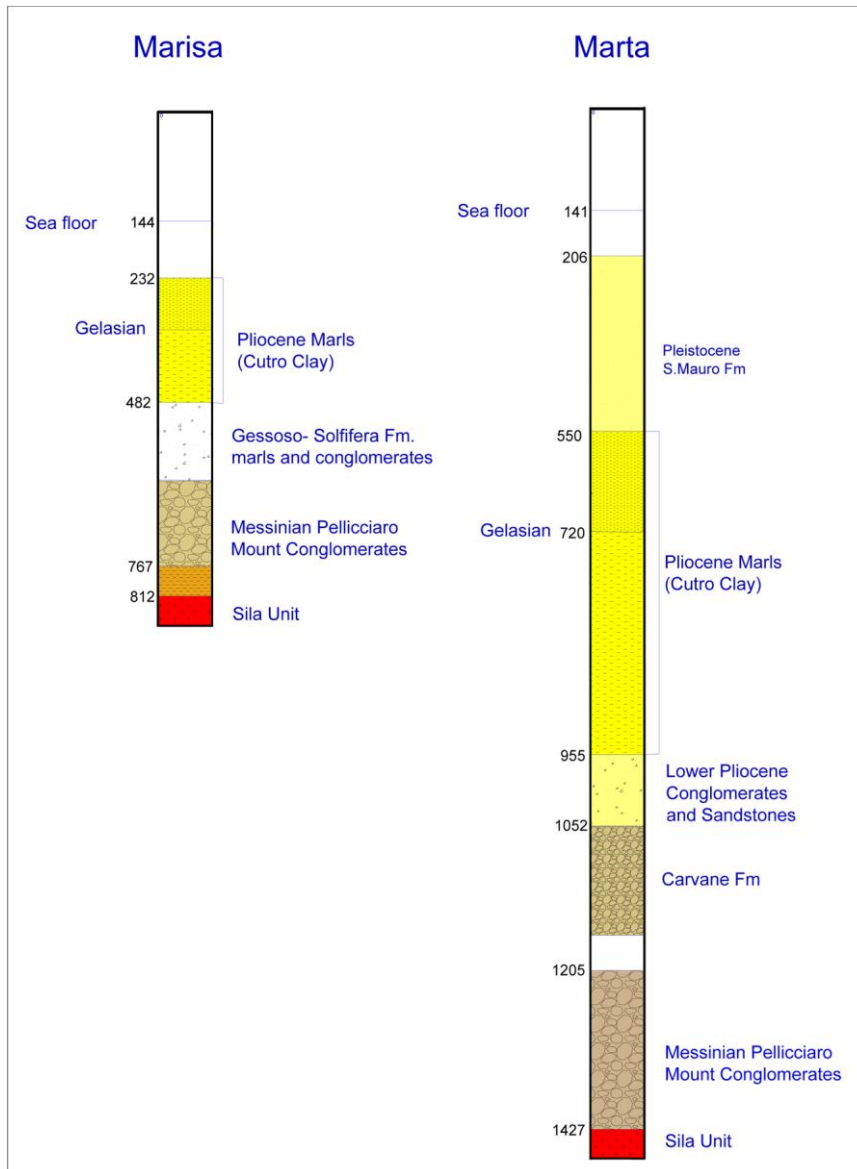
515 and Pliocene marls, and unconformity between Pliocene and Pleistocene deposits; c) Pliocene weakly sandstones and  
 516 mudstones outcropping in the area; d) Lower Pleistocene mixed sands and sandstones showing foresets organized in  
 517 trough cross-strata close to Pianopoli Village; e) Erosional contact between Lower Pleistocene biocalcarenes and sand-  
 518 wave deposits and Middle Upper Pleistocene Marine Terrace, *inset e'*) Detail of Middle- Upper Pleistocene Marine  
 519 Terrace outcrop.

520



521

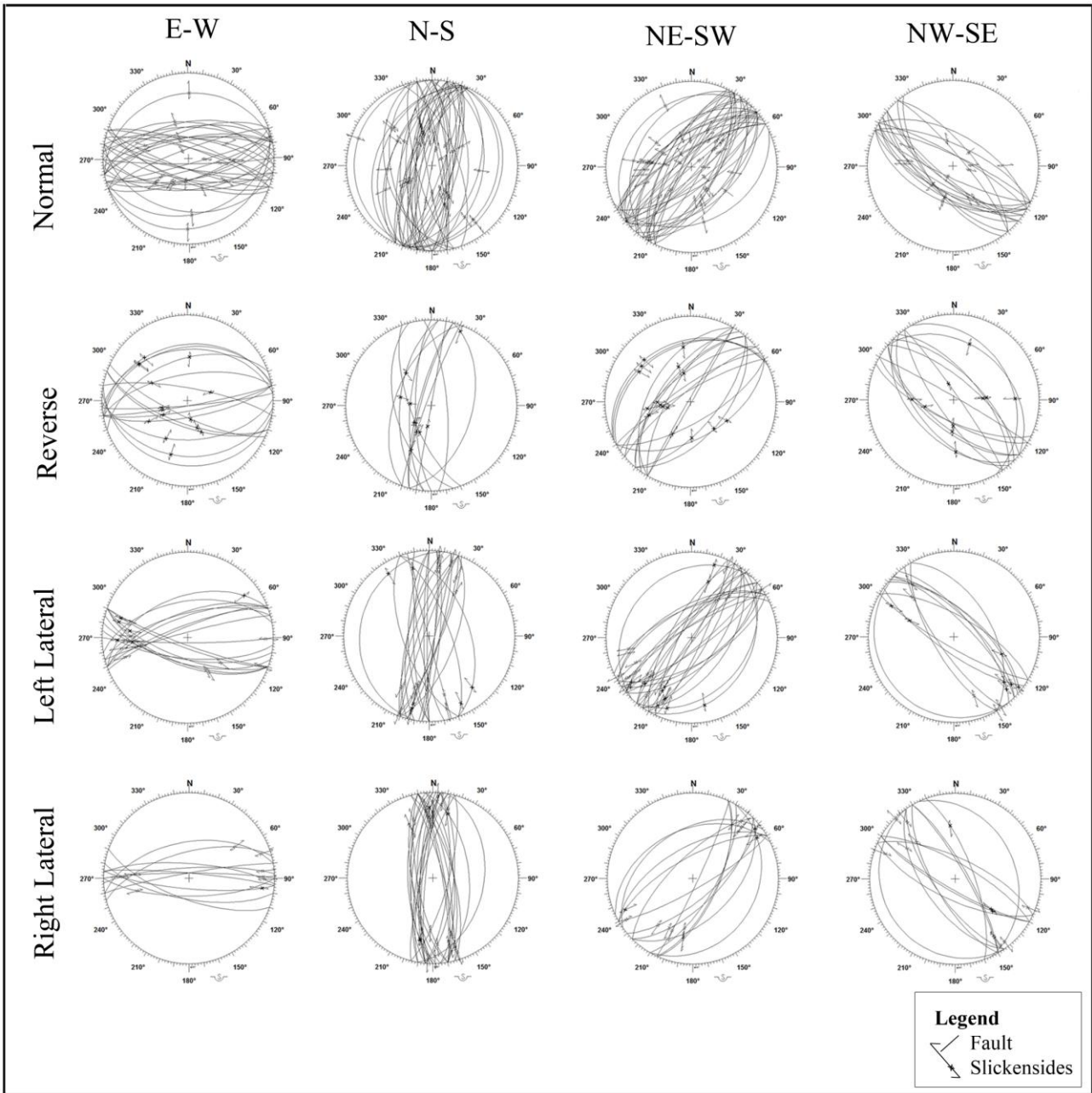
522 Figure 5: Location map of the multichannel seismic (MCS) profiles (light green lines; part of the ISTEGE project),  
 523 Sparker profiles (blue lines; part of the VP 87 cruise I.G.M. Geological Marine Institute of Bologna onboard the RV  
 524 Bannock 1987), ViDEPI multichannel profiles (green lines; ViDEPI project; [unmig.sviluppoeconomico.gov.it/videpi/](http://unmig.sviluppoeconomico.gov.it/videpi/)),  
 525 and Eni wells (violet dots), and the 35 stations of structural measurements (blue dots) studied in the western Catanzaro  
 526 Trough and in the Sant'Eufemia Gulf (SE Tyrrhenian Sea).



527

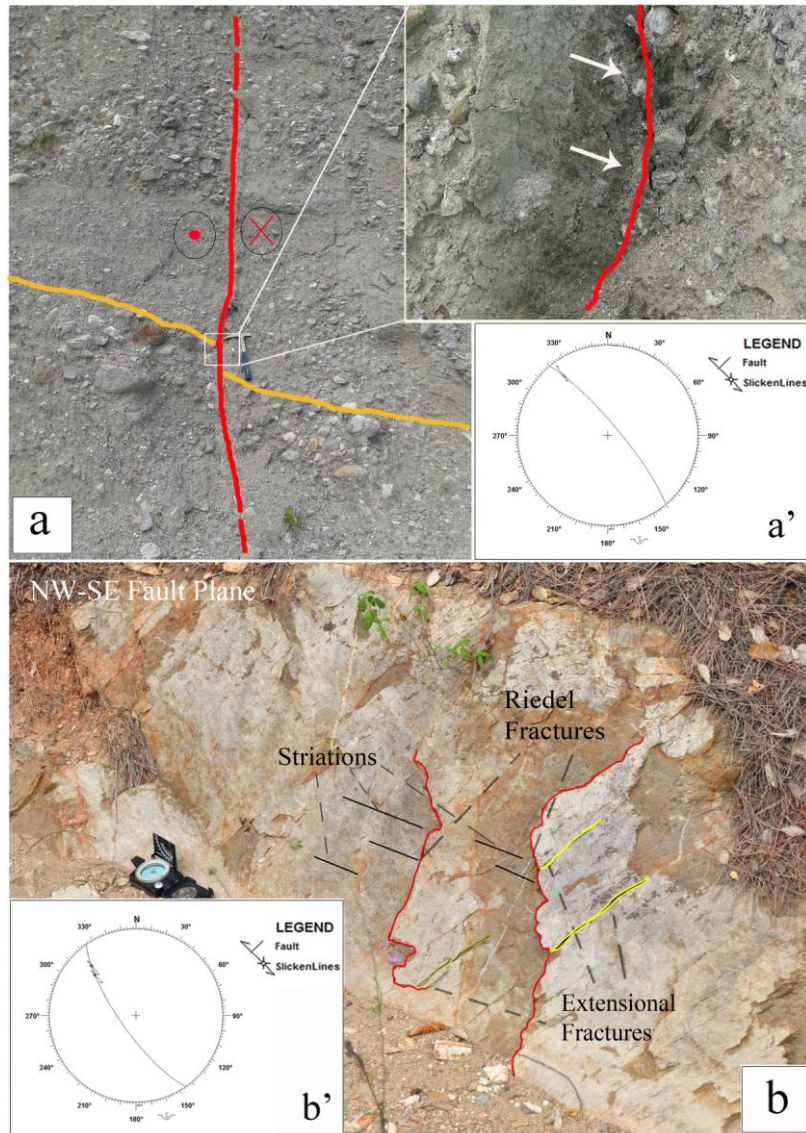
528

Figure 6: Stratigraphic columns reconstructed by using the Eni wells.



529

530 Figure 7: Structural data of the western portion of Catanzaro Trough which show orientation and kinematics of fault  
 531 planes.



532

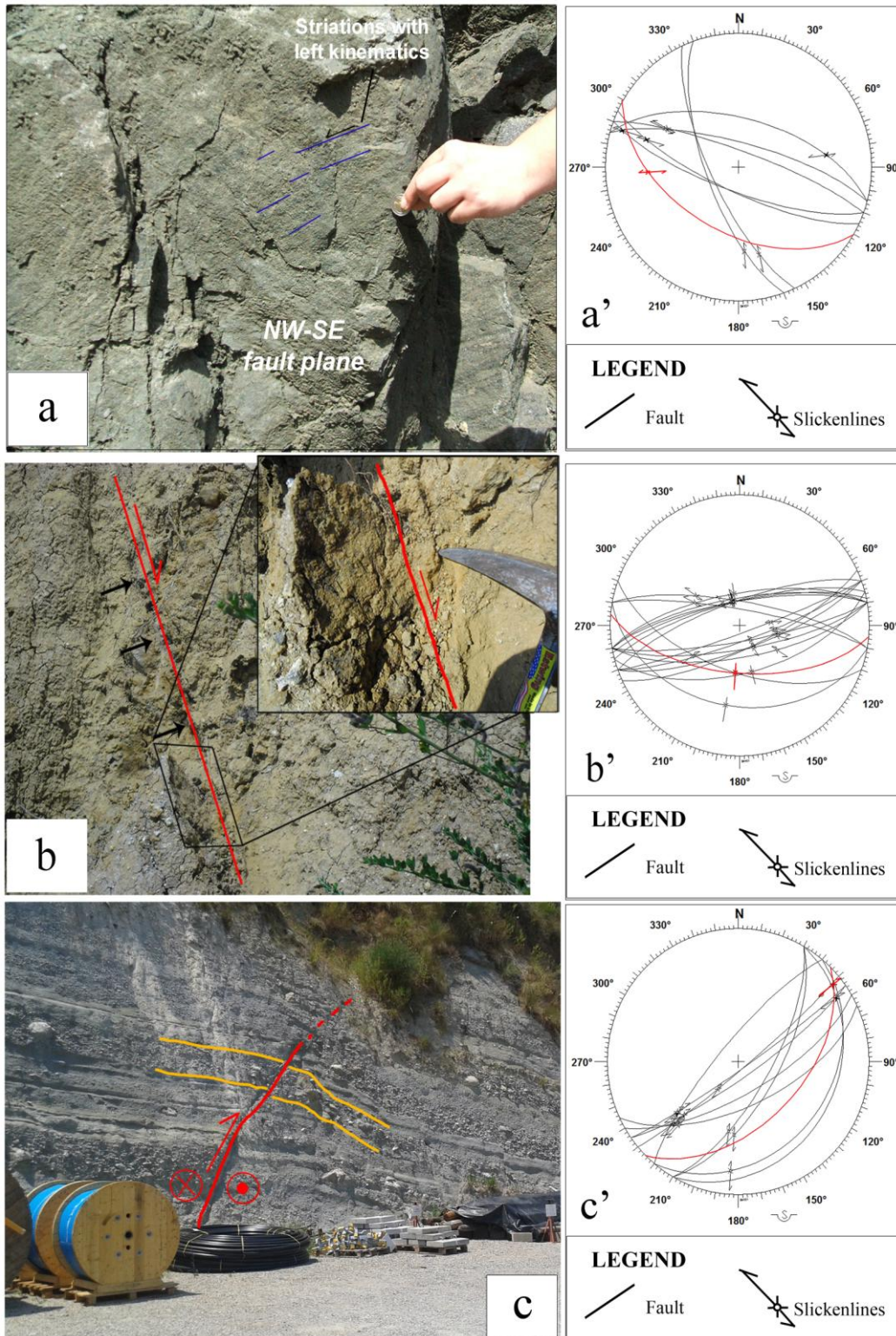
533

534

535

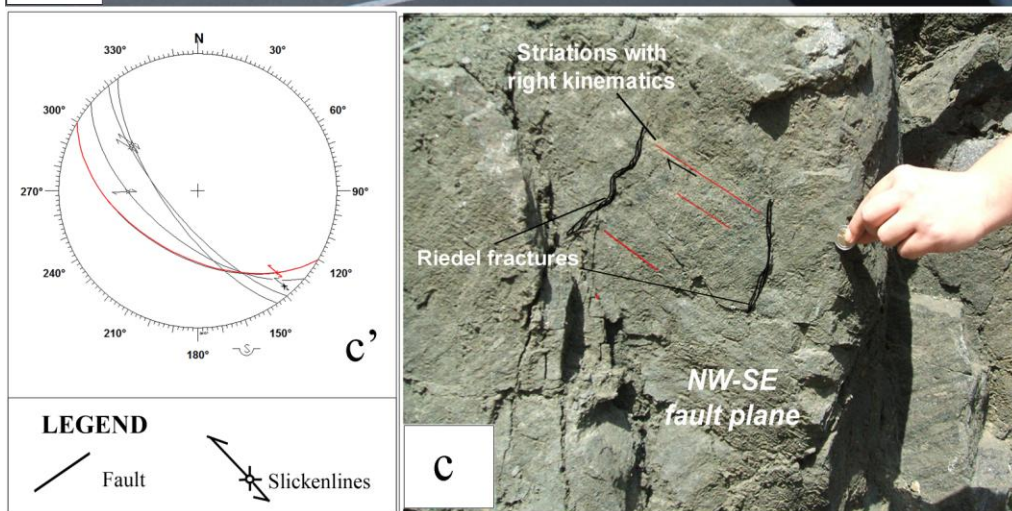
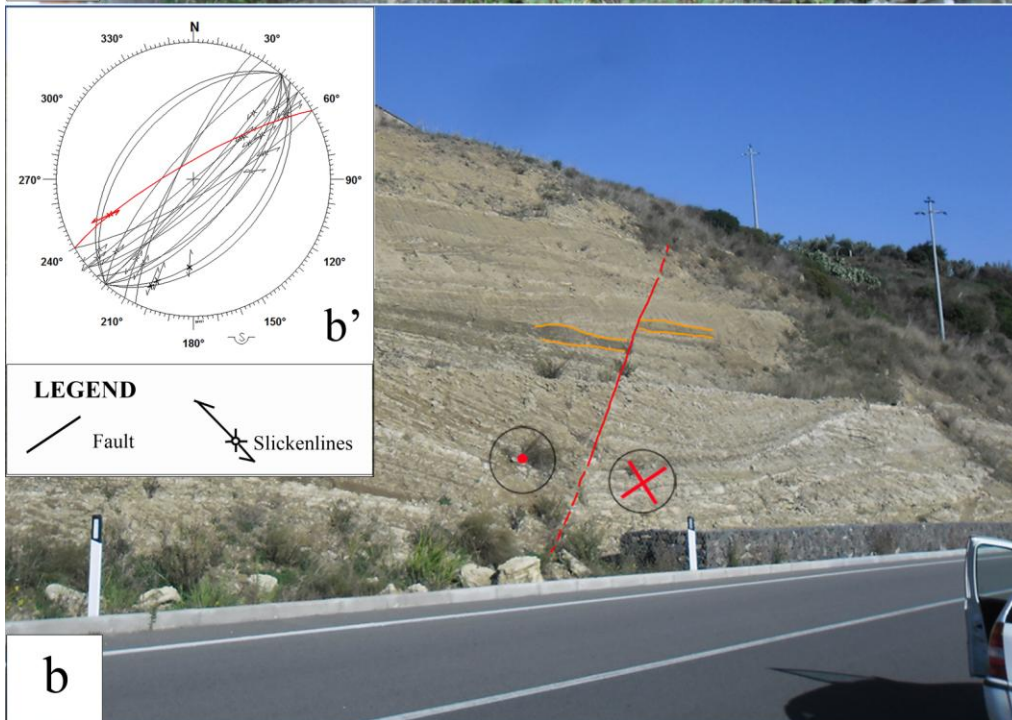
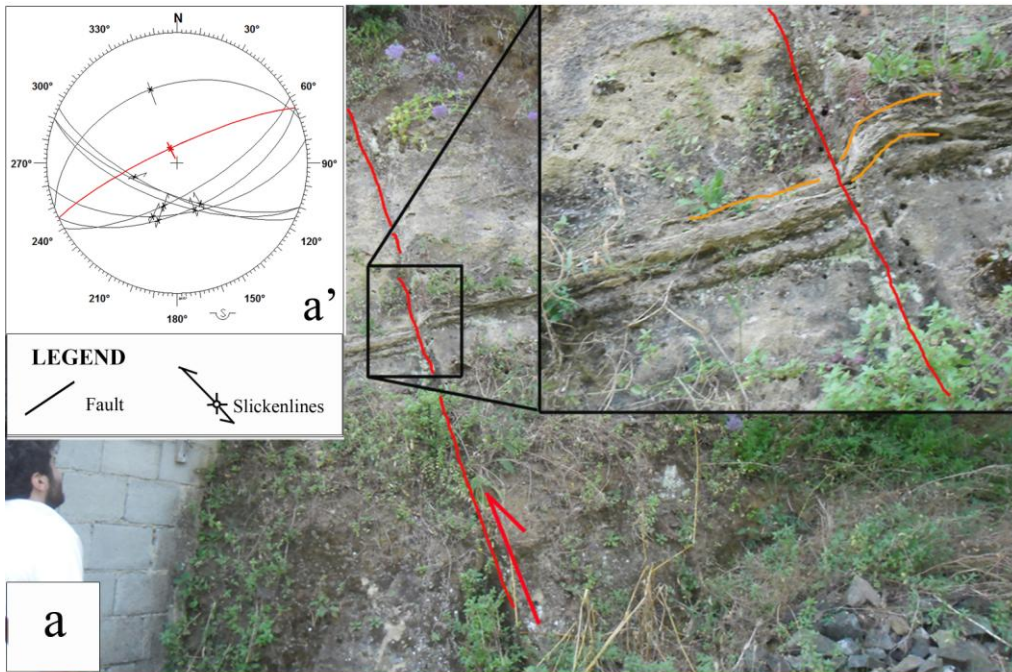
536

Figure 8: NW-SE left-lateral strike-slip fault planes dislocating a) Messinian conglomerate with stereographic plot in inset a' (detail in the box shows white arrows related to the left lateral kinematics) and b) basement rocks close to the Nicastro town with stereographic plots in inset b': red, black and yellow lines represent Riedel fractures, extensional fractures and striations, respectively

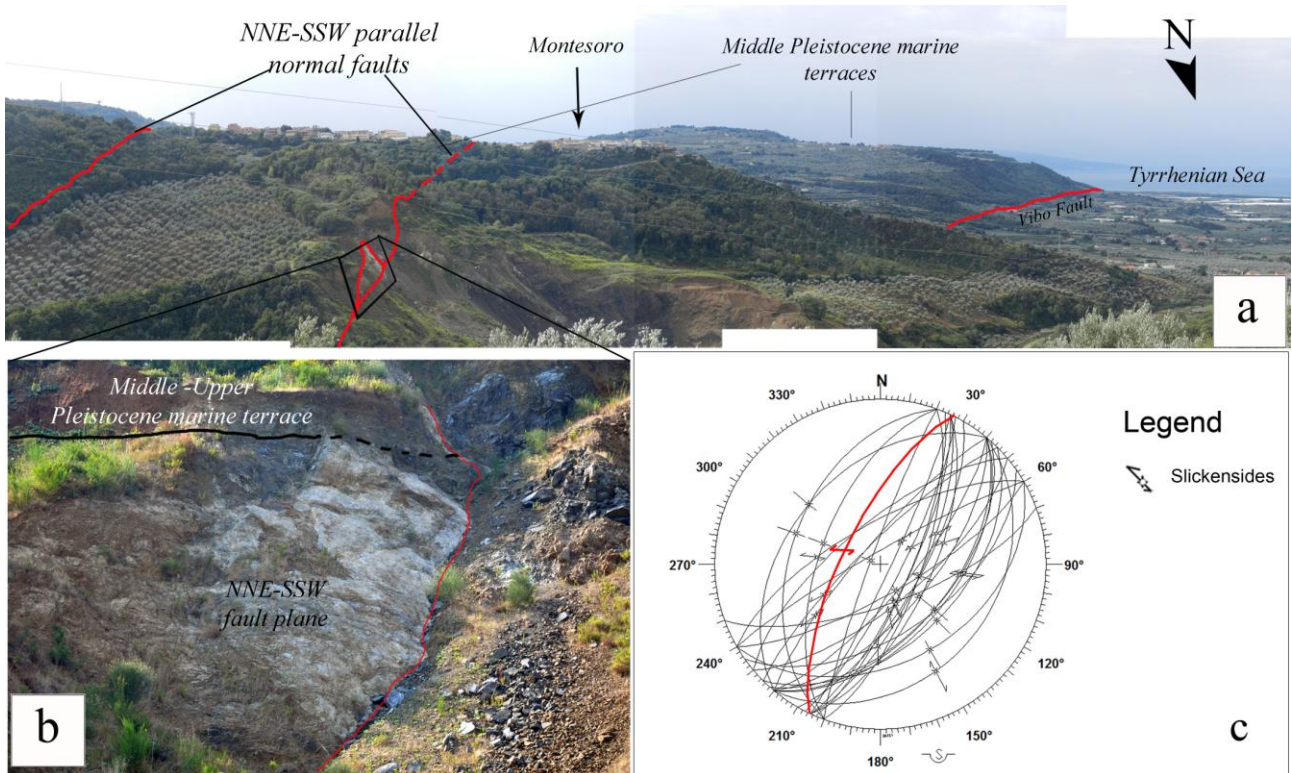


537

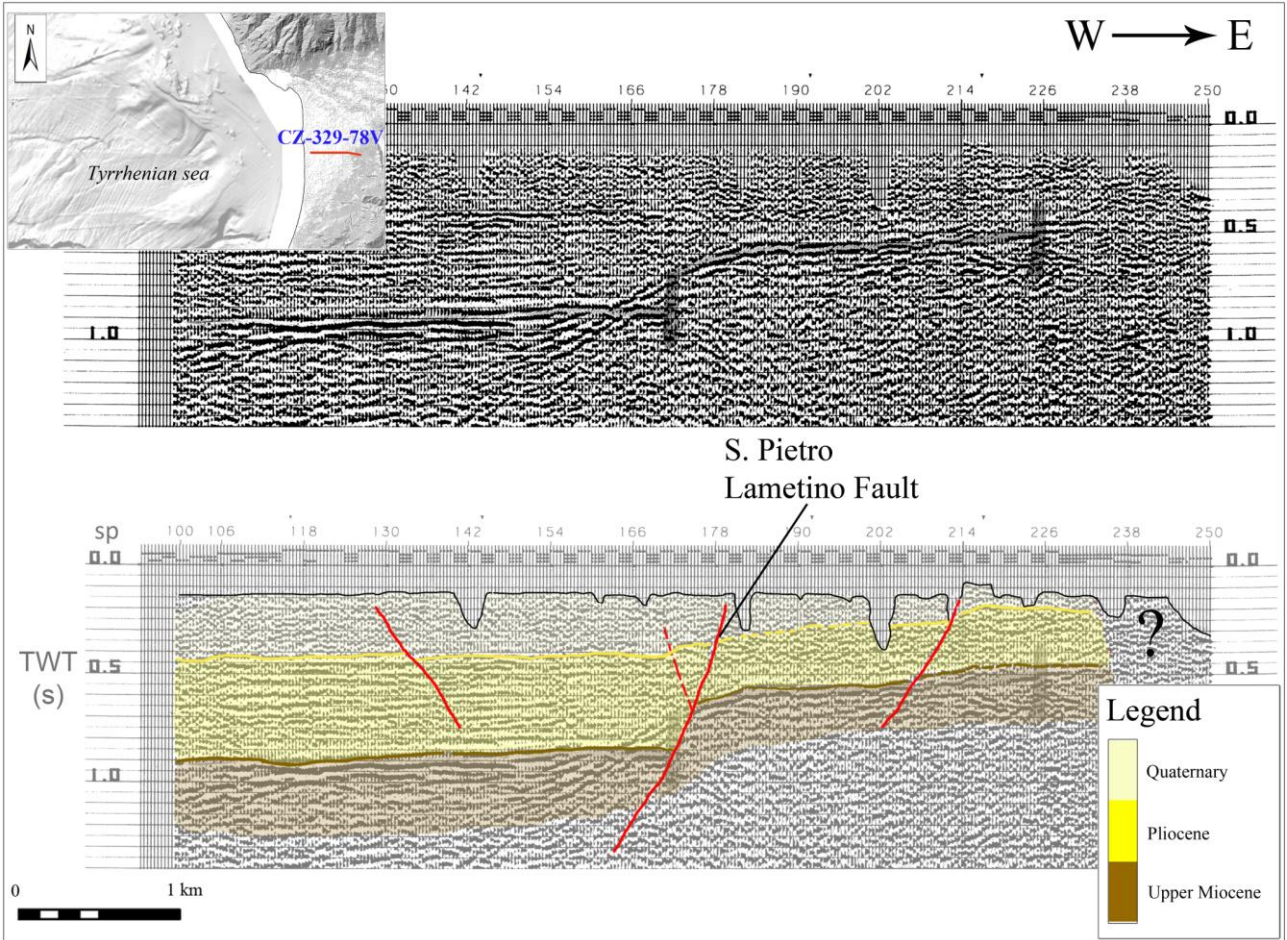
538 Figure 9: Fault associations offsetting the Upper Miocene -Pliocene deposits. a) NW-SE strike-slip faults showing left-  
 539 lateral kinematics (blue lines), inset a') stereographic plot related to the NW-SE left lateral kinematics, red fault shows  
 540 the kinematics in figure a; b) WNW-ESE and WSW-ENE extensional faults systems, inset b') stereographic plot related  
 541 to the WNW-ESE normal kinematics, red fault shows the kinematics in figure b, c) NE-SW right-lateral strike-slip,  
 542 inset c') stereographic plot related to the NE-SW right lateral kinematics, red fault shows the kinematics in figure c.



544 Figure 10: a) WNW-ESE reverse fault, inset a' ) stereographic plot related to the WNW-ESE reverse kinematics, red  
 545 fault shows the kinematics in figure a; b) NE-SW left-lateral fault, inset b' ) stereographic plot related to the NE-SW  
 546 left-lateral kinematics, red fault shows the kinematics in figure b; and c) NW-SE strike-slip faults showing right lateral  
 547 kinematics (red lines), inset c' ) stereographic plot related to the NW-SE right lateral kinematics, red fault shows the  
 548 kinematics in figure c  
 549



550  
 551 Figure 11: a) Overview of southwestern margin of the study area, b) Evidences for recent fault activation along tectonic  
 552 contact between basement rocks and Pleistocene Marine Terraces, inset c' ) stereographic projection of the NE-SW  
 553 normal faults (red line represents the fault kinematics in Fig. 11b).

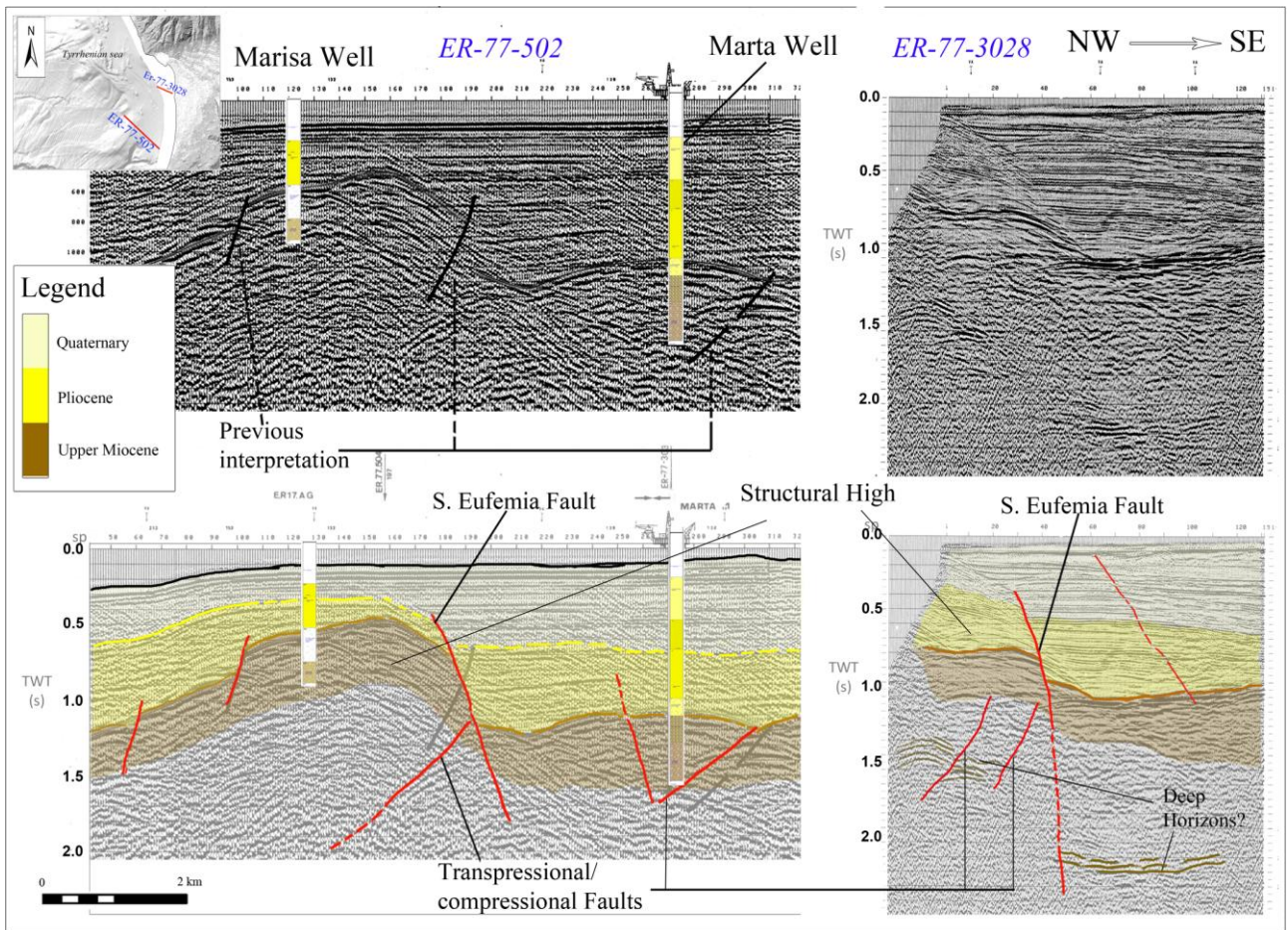


554

555 Figure 12: CZ-329-78 ViDEPI seismic profile (above) and the same with the interpretation (below), location is marked

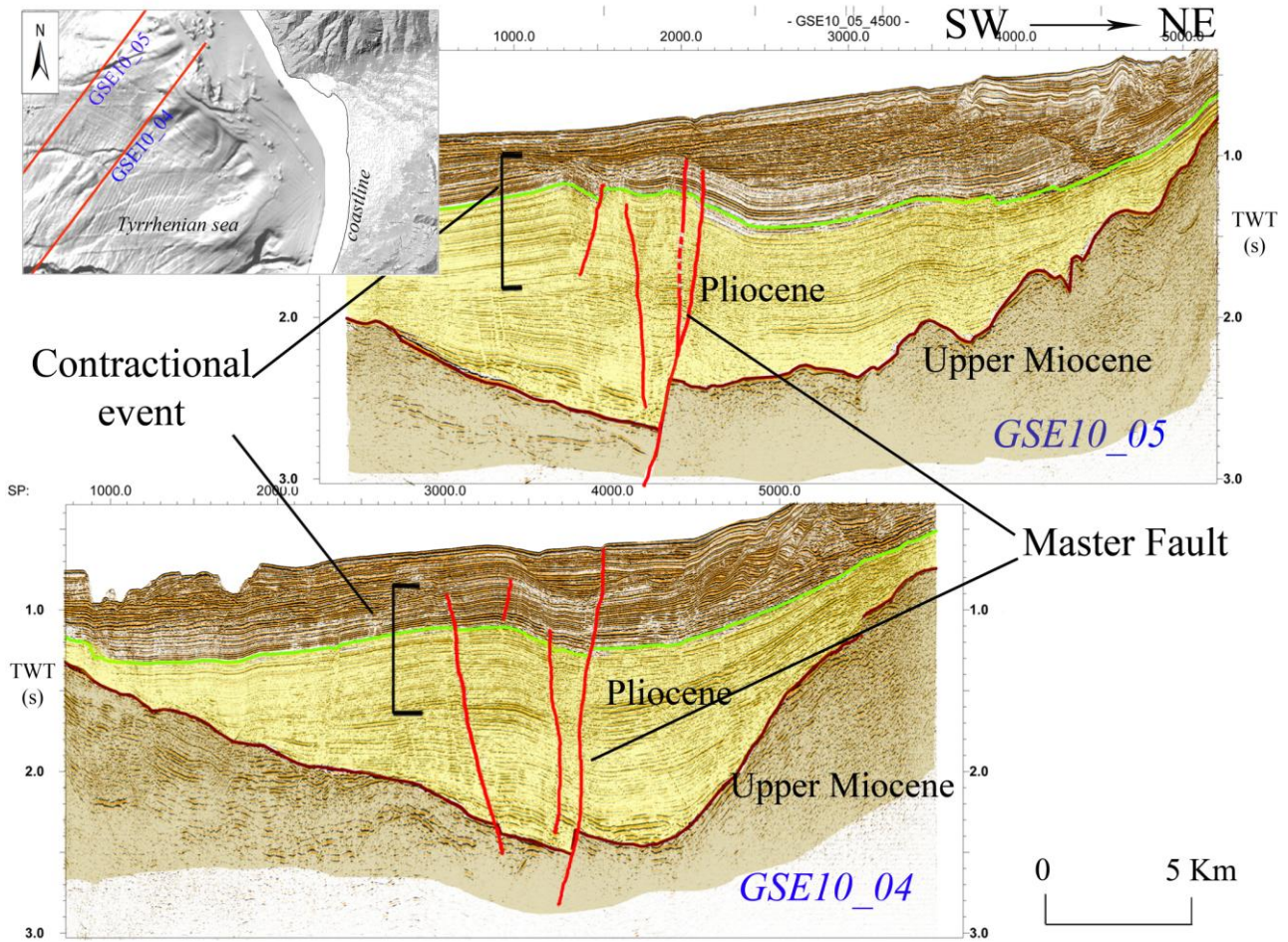
556 with a red line in the box. Brown line marks the top of Miocene; Yellow line marks the Pliocene-Pleistocene transition.





557

558 Figure 13: Two ViDEPI seismic profiles (above): the ER-77-502, on the left; and the ER-77-3028, on the right, location  
 559 is marked with a red line in the box. On the interpretation (below): brown line marks the top of Miocene; yellow line  
 560 marks the Pliocene-Pleistocene transition.



561

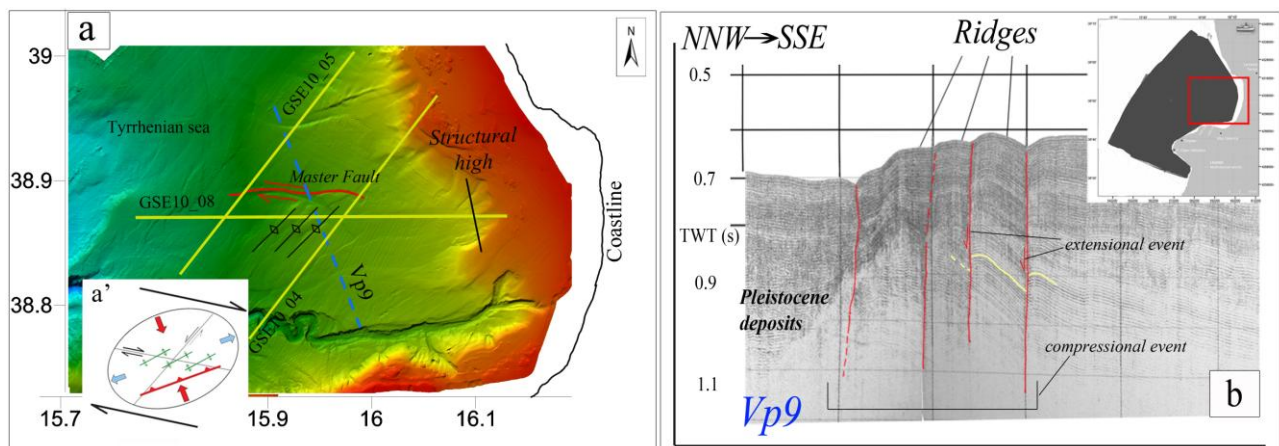
562

563

564

565

Figure 14: MCS profiles acquired in the frame of ISTEGE project, location is marked with a red line in the box. The green and brown reflectors represent the top of the Pliocene and Miocene, respectively, whereas the red lines represent the main recognized faults. The interpretation has been made by using the Kingdom software (HIS Global Inc.).



566

567

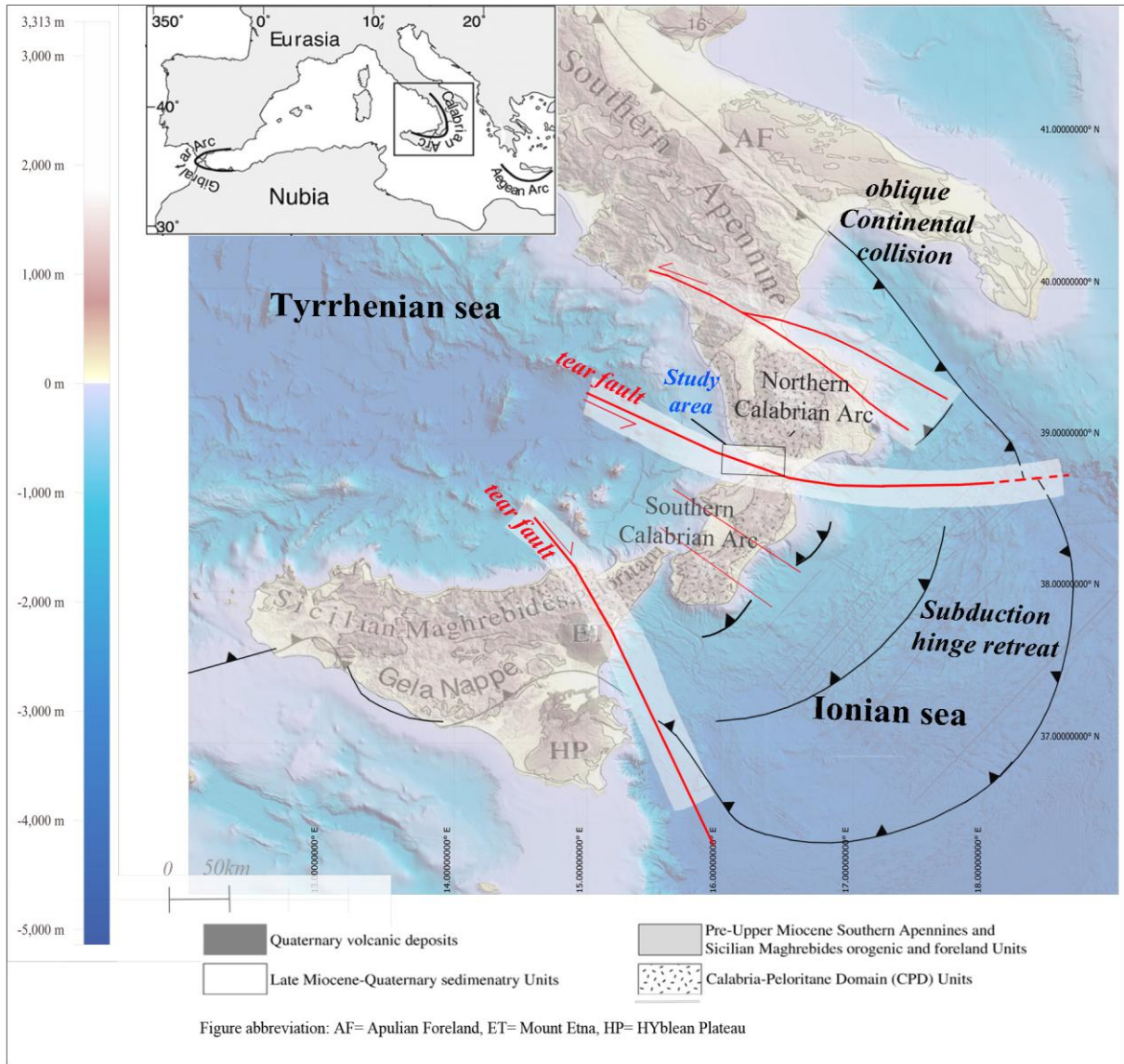
568

Figure 15: a) High-resolution morpho-bathymetric map showing three small ridges, indicated with black fold axes and located in center of the Sant'Eufemia Gulf. Blue dotted and yellow lines represent Vp9 Sparker and MCS profiles,

569 respectively, inset a') a sketch of destral stress regime, applied in the area related to Master Fault kinematics; b) Vp9

570 Sparker seismic profile imaging the three small tectonic ridges.

571

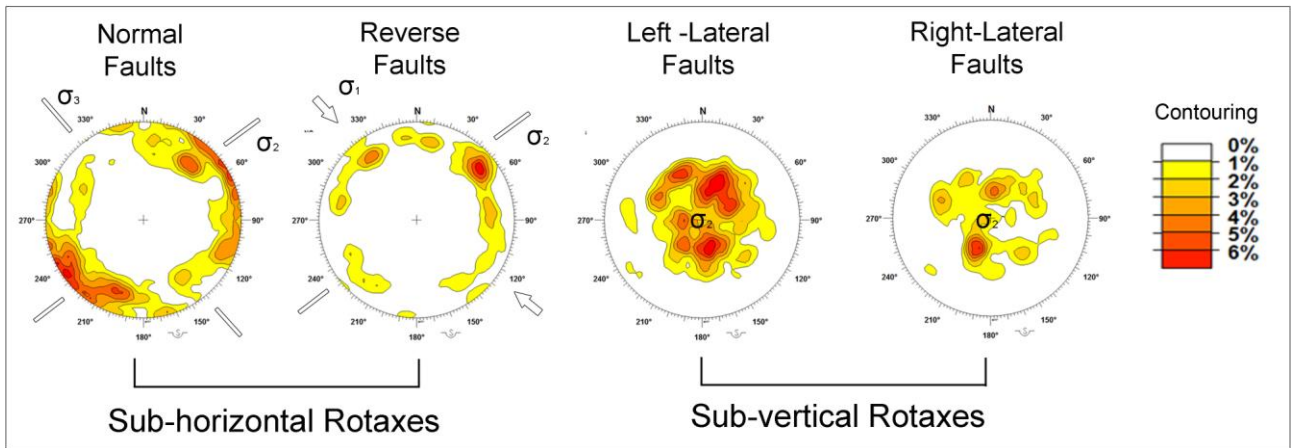


572

573 Figure 16: Western Mediterranean subduction system (inspired from Van Dijk et al., 2000; Guarnieri et al., 2006;

574 Mattei et al., 2007; Neri et al., 2009; Cuffaro et al., 2011).

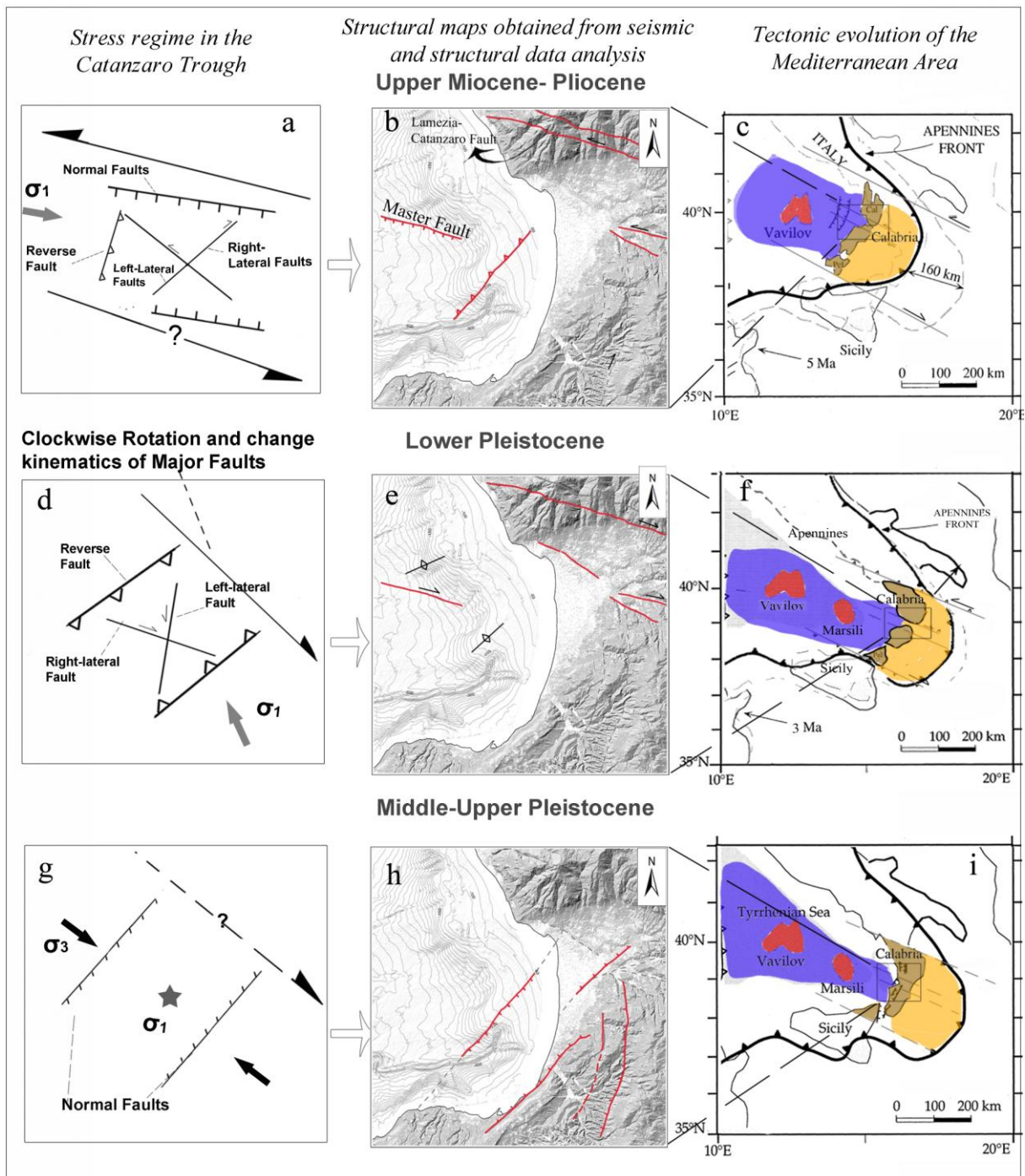
575



576

577

Fig. 17: Contours of the rotaxes used to discriminate the different deformational events.

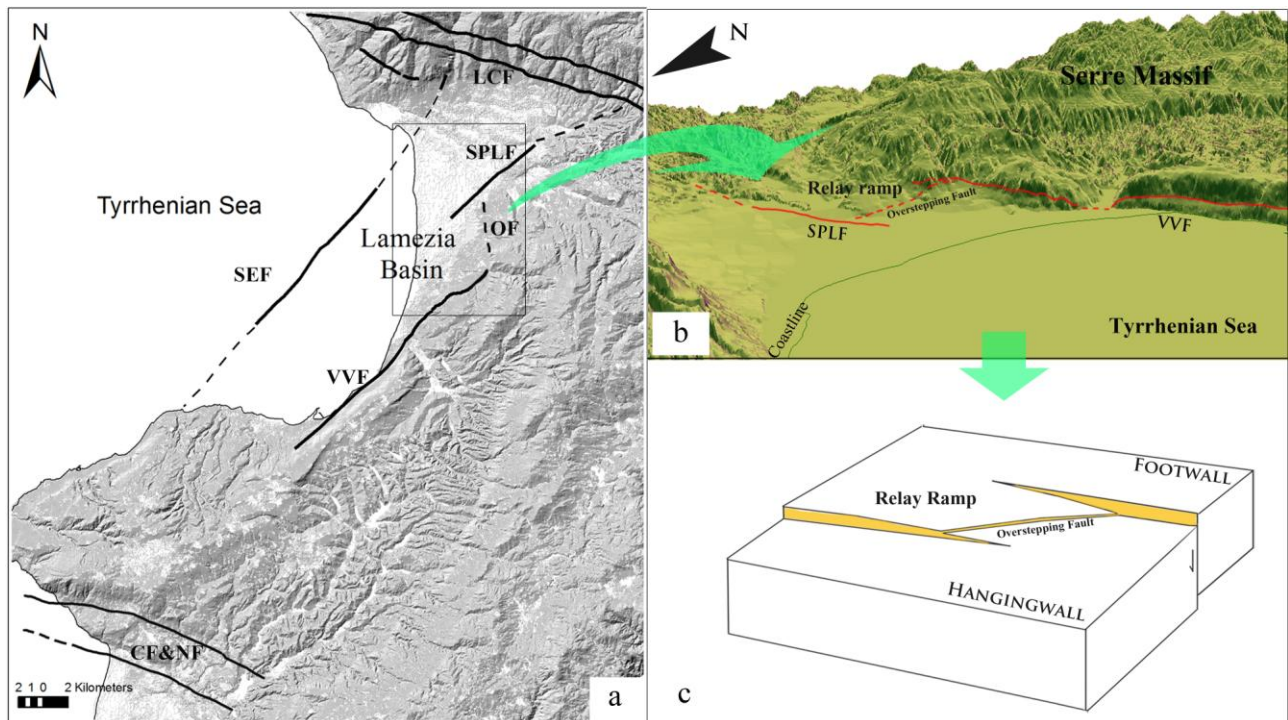


578

579 Figure 18: Palinspastic reconstruction of Catanzaro Trough and of Southern Apennine system; for more details, see the

580

text (inspired in Gueguen et al., 1998; Zecchin et al., 2015).



581

582 Figure 19: a) Structural map of Major Faults: (LCF) Lamezia –Catanzaro Fault, (SEF) Sant’Eufemia Fault, (SPLF) San  
 583 Pietro Lametino Fault, (OF) Overstepping Fault, (VVF) Vibo Valentia Fault, (CF&NF) Coccorino & Nicotera Fault. b)  
 584 Hillshade of morphological map along Vibo Valentia and San Pietro Lametino Faults, c) Schematic representation of  
 585 relay ramp (Peacock & Parfitt 2002).

586

## 587 Reference

- 588 Allen, M.B., MacDonald, D.I.M., Xun, Z., Vincent, S.J., Brouet- Menzies, C., 1998. Transensional deformation in the  
 589 evolution of the Bohai Basin, northern China, in: Holdsworth, R.E., Strachan, R.A., Dewey, J.F. (Eds.),  
 590 Continental Transpressional and Transensional Tectonics. Geological Society of London Special Publication,  
 591 135, pp. 215–229.
- 592 Amodio-Morelli, L., Bonardi, G., Colonna, V., Dietrich, D., Giunta, G., Ippolito, F., Liguori, V., Lorenzoni, S.,  
 593 Paglionico, A., Perrone, V., Piccarreta, G., Russo, M., Scandone, P., Zanettin-Lorenzoni, E., Zuppetta, A.,  
 594 1976. L’arco Calabro-Peloritano nell’orogene appenninico Maghrebite (The Calabrian-Peloritan Arc in the  
 595 Apennine-Maghrebite orogen). Memorie della Societ`a Geologica Italiana 17, 1–60.
- 596 Angi, G., Cirrincione, R., Fazio, E., Fiannacca, P., Ortolano, G., Pezzino, A., 2010. Metamorphic evolution of preserved  
 597 Hercynian crustal section in the Serre Massif (Calabria- Peloritani Orogen, southern Italy): Lithos, v. 115, no.  
 598 1–4, p. 237–262.

- 599 Barone, M., Dominici, R., Muto, F., Critelli, S., 2008. *Detrital mode in late Miocene wedge-top basin northeastern*  
600 *Calabria, Italy: compositional record of wedge – top partitioning*. Journal of sedimentary Research, **78**, 693-  
601 711.
- 602 Beauchamp W, Allmendinger RW, Barazangi M. 1999. Inversion tectonics and the evolution of the High Atlas  
603 Mountains, Morocco, based on a geological-geophysical transect. Tectonics 18(2): 163–184.
- 604 Beck, M. E., Jr., 1983. On the mechanism of tectonic transport in zones of oblique subduction. Tectonophysics, 93, 1–  
605 11.
- 606 Bianca, M., Catalano, S., De Guidi, G., Gueli, A.M., Monaco, C., Ristuccia, G.M., Stella, G., Tortorici, G., Tortorici,  
607 L., Troja, S.O., 2011. Luminescence chronology of Pleistocene marine terraces of Capo Vaticano Peninsula  
608 (Calabria, Southern Italy). Quaternary International 232, 114-121.
- 609 Billi, A., R. Funiciello, L. Minelli, C. Faccenna, G. Neri, B. Orecchio, D. Presti (2008), On the cause of the 1908  
610 Messina tsunamis, southern Italy, Geophys. Res. Lett., 35, L06301, doi:10.1029/2008GL033251.
- 611 Bonardi, G., Cavazza, W., Perrone, V., Rossi, S., 2001. Calabria-Peloritani Terrane and Northern Ionian Sea. In:  
612 Martini, L.P., Vai, G.B. (Eds.), Anatomy of an Orogen: The Apennines and Adjacent Mediterranean Basins.  
613 Kluwer Academic Publication, pp. 287–306.
- 614 Bordoni, P., Valensise, G., 1998, Deformation of the 125 ka marine terrace in Italy: tectonic implications. In: Stewart,  
615 I.S. and Vita Finzi, C. (eds), Late Quaternary Coastal Tectonics, Geological Society, London, Special  
616 Publications 146, pp. 71–110.
- 617 Bousquet J.C. 1963. Contribution à l' étude de roches verte du nord de la Calabre e du sud de la Lucanie. These the  
618 3ème Cycle Faculté de Science de l'Université Paris. pp. 145.
- 619 Brutto, F., Muto, F., Loreto, M.F., Tripodi, V., Critelli, S., 2015. Plio-Quaternary structural evolution of the western  
620 Catanzaro Trough (Calabria, South Italy), Conference abstract and poster presented in EGU General Assembly  
621 2015.
- 622 Calò, M., Dorbath, C., Luzio, D., Rotolo, S.G., D'Anna, G. 2012. Seismic velocity structures of southern Italy from  
623 tomographic imaging of the Ionian slab and petrological inferences. Geophysical Journal International.  
624 <http://dx.doi.org/10.1111/j.1365-246X.2012.05647.x>.
- 625 Cavazza, W., Ingersoll, R.V., 2005. Detrital modes of the Ionian forearc basin fill (Oligocene-Quaternary) reflect the  
626 tectonic evolution of the Calabria-Peloritani terrane (southern Italy). J. Sed. Res., 75, 268–279.
- 627 Cavazza, W., Decelles, P.G., 1998. Upper Messinian siliciclastic rocks in southeastern Calabria (S Italy): Paleotectonic  
628 and eustatic implications for the evolution of the central Mediterranean region. Tectonophysics 298, pp. 223–  
629 241 Chiarella, D., Longhitano, S.G. and Muto, F. 2012a. Sedimentary features of the Lower Pleistocene mixed

630 siliciclastic-bioclastic tidal deposits of the Catanzaro Strait (Calabrian Arc, south Italy). *Rend. Soc. Geol. Ital.*,  
631 21, pp. 919–920.

632 Cavazza, W., Blenkinsop, J., De Celles, P.G., Patterson, R.T., Reinhardt, E.G. 1997. Stratigrafia e sedimentologia della  
633 sequenza sedimentaria oligocenico–quaternaria del bacino calabro–ionico. *Bollettino della Società Geologica*  
634 *Italiana* 116, pp. 51–77.

635 Chiarella, D., Longhitano, S.G., Muto, F. 2012. Sedimentary features of the Lower Pleistocene mixed siliciclastic-  
636 bioclastic tidal deposits of the Catanzaro Strait (Calabrian Arc, south Italy). *Rendiconti online Società*  
637 *Geologica Italiana* 21, pp. 919–920.

638 Chiarella, D., 2011. Sedimentology of Pliocene–Pleistocene mixed (lithoclastic-bioclastic) deposits in southern Italy  
639 (Lucanian Apennine and Calabrian Arc): depositional processes and palaeogeographic frameworks  
640 [unpublished PhD thesis]: University of Basilicata, Potenza, 216 pp.

641 Cianflone, G., Dominici, R., 2011. Physical stratigraphy of the upper Miocene sedimentary succession in the  
642 northeastern Catanzaro Through (Central Calabria, Italy). *Rend. Soc. Geol. Ital.*, 17, 63–69.

643 Colella, A. 1995. Sedimentation, deformational events and eustasy in the perityrrhenian Amantea Basin: preliminary  
644 synthesis. *Giornale di Geologia* 57, pp. 179–193.

645 Critelli, S., Muto, F., Tripodi, V., Perri, F., 2011. Relationships between lithospheric flexure, thrust tectonics and  
646 stratigraphic sequences in foreland setting: the southern Apennines foreland basin system, Italy. In: Schattner,  
647 U. (Ed.), *New Frontiers in Tectonic Research—at the Midst of Plate Convergence*. InTech Open Access  
648 Publisher, pp. 121–170.

649 Critelli, S., Muto, F., Tripodi, V., Perri, F., 2013. Link between thrust tectonics and sedimentation processes of  
650 stratigraphic sequences from the southern Apennines foreland basin system, Italy. *Rend. Soc. Geol. Ital.*, 25,  
651 21–42.

652 Cucci, L., Tertulliani, A., 2006. I terrazzi marini nell'area di Capo Vaticano (arco calabro): solo un record di  
653 sollevamento regionale o anche di deformazione cosismica? *Il Quaternario* 19, 89–101.

654 Cunningham, W.D., Mann, P., 2007. *Tectonics of Strike-Slip Restraining and Releasing Bends*. Geological Society,  
655 London, Special Publications, 290, 1–12. DOI: 10.1144/SP290.

656 Cuffaro M., Riguzzi F., Scrocca D., Doglioni C., 2011. Coexisting tectonic settings: the example of the southern  
657 Tyrrhenian Sea. *Int J Earth Sci (Geol Rundsch)* DOI 10.1007/s00531-010-0625-z

658 D'Agostino, N., Selvaggi, G., 2004. Crustal motion along the Eurasia– Nubia plate boundary in the Calabrian Arc and  
659 Sicily and active extension in the Messina Straits from GPS measurements. *J. Geophys. Res.* 109, B11402.  
660 doi:10.1029/2004JB002998.



- 661 Del Ben, A., Barnaba, C., Taboga, A., 2009. Strike-slip systems as the main tectonic features in the Plio-Quaternary  
662 kinematics of the Calabrian Arc. *Marine Geophysical Researches* 29, pp. 1–12.
- 663 De Paola, N., Mirabella, F., Barchi, M.R., Burchielli, F., 2006. Early orogenic normal faults and their reactivation  
664 during thrust belt evolution: the Gubbio Fault case study, Umbria-Marche Appennines (Italy). *Journal of*  
665 *structural Geology* 28, 1948-1957.
- 666 De Paola, N., Holdsworth, R.E., McCaffrey, K.J.W., Barchi, M.R., 2005. Partitioned transtension: an alternative to  
667 basin inversion models. *Journal of Structural Geology* 27, pp. 607-625.
- 668 Dewey, J.F., Helman, M.L., Turco, E., Hutton, D.H.W., Knott, S., 1989. Kinematics of the Western Mediterranean, in  
669 *Alpine Tectonics*, eds Coward, M. P. & Dietrich, D., *Geol. Soc. Lond. Spec. Publ.*, 45, 265–283.
- 670 Diament, M., Harjono, H., Karta, K., Deplus, C., Dahrin, D., Zen, M.T. Jr., Gerard, M., Lassal, M., Martin, M., and  
671 Malod, J. 1992. Merittawai fault zone off Sumatra: a new key to the geodynamics of western Indonesia,  
672 *Geology*, 20, 259-262.
- 673 Di Stefano, A., Lentini R., 1995. Ricostruzione stratigrafica e significato paleotettonico dei depositi Plio-Pleistocenici  
674 del margine tirrenico tra Villafranca Tirrena e Faro (Sicilia nord-orientale). *Studi Geologici Camerti*, Volume  
675 Speciale 2, pp. 219–237.
- 676 Dumas, B., Guerey, P., Lhenaff, R., Raffy J.; 1987- Rates of uplift as shown by raised Quaternary shorelines in  
677 southern Calabria (Italy). *Z. Geomorphol. N.F.*, 63, 119-132.
- 678 **Fabbricatore, D., Robustelli, G., Muto, F., 2014. Facies analysis and depositional architecture of shelf-type deltas in the**  
679 **Crati Basin (Calabrian Arc, south Italy). *Ital. J. Geosci.* 133, 131–148.**
- 680 Faccenna, C., Civetta, L., D'Antonio, M., Funiciello, F., Margheriti, L., Piromallo C., 2005. Constraints on mantle  
681 circulation around the deforming Calabrian slab. *Geophys. Res. Lett.*, 32, L06311,  
682 doi:10.1029/2004GL021874.
- 683 Ferranti, L., Oldow, J.S., D'Argenio, B., Catalano, R., Lewis, D., Marsella, E., Avellone G., Maschio, L., Pappone, G.,  
684 Pepe, F., Sulli, A., 2008. Active deformation in Southern Italy, Sicily and southern Sardinia from GPS  
685 velocities of the Peri-Tyrrhenian Geodetic Array (PTGA). *Bollettino della Società Geologica Italiana*, Italian  
686 *Journal of Geosciences* 127, 299-316.
- 687 Ferrini, G., Testa, G., 1997. La successione miocenico superiore della Stretta di Catanzaro, dati preliminari. In: Abstracts  
688 of the Gruppo di Sedimentologia del CNR (Ed. S. Critelli), Annual Meeting, 13–17 October, Arcavacata di  
689 Rende, CS, pp. 53–55.
- 690 Finetti I., Del Ben A., 1986. Geophysical study of the Tyrrhenian opening . *Boll. Geofis. Teor. Appl.*, 28: 75-155.

691 Fitch T. J., 1972. Plate convergence, transcurrent faults, and internal deformation adjacent to Southeast Asia and the  
692 western Pacific. *Journal of Geophysical Research*. V. 77, pp. 4432- 4460.

693 Fossen, H., 2010. *Structural geology*. Cambridge University press. Pp. 463.

694 Galli, P., Scionti V., Spina, V., 2007. New paleoseismic data from the Lakes and Serre faults: seismotectonic  
695 implications for Calabria (Southern Italy). *Ital. J. Geosci.*, 126, pp. 347-364.

696 Galli, P., Bosi, V., 2003. Catastrophic 1638 earthquakes in Calabria (southern Italy): new insights from  
697 palaeoseismological investigation. *Journal of Geophysical Research*, 108 (B1).

698 Gasparini, C., Iannacone, G., Scandone, P., Scarpa, R. 1982. Seismotectonics of the Calabrian Arc. *Tectonophysics* 82,  
699 pp. 267–286.

700 Ghisetti, F., 1981. Upper Pliocene-Pleistocene uplift rates as indicators of neotectonic pattern: an example from  
701 southern Calabria (Italy). *Zeitschrift fur Geomorphologie*, 40, pp. 93–118.

702 Ghisetti, F., 1979. Evoluzione neotettonica dei principali sistemi di faglie della Calabria centrale: *Bolletino Società*  
703 *Geologica Italiana*, 98, pp. 387–430.

704 Ghisetti, F., Vezzani L., 1982. Strutture tensionali e compressive indotte da meccanismi profondi lungo la linea del  
705 Pollino (Appennino meridionale). *Bollettino della Societa Geologica Italiana*, 101(3), pp. 385-440.

706 Govers, R., Meijer, P., Rijgsman, W., 2009. Regional isostatic response to Messinian Salinity Crisis events.  
707 *Tectonophysics*, 463, pp. 109–129.

708 Guarnieri, P., 2006. Plio-Quaternary segmentation of the south Tyrrhenian forearc basin. *Int. J. Earth Sci.*, 95, pp. 107-  
709 118.

710 Gueguen, E., Doglioni, C., Fernandez, M., 1998. On the post-25 Ma geodynamic evolution of the western  
711 Mediterranean. *Tectonophysics*, 298, pp. 259-269.

712 Hanuš, V., Špičák, A., Vaněk J., 1996. Sumatran segment of the Indonesian subduction zone: morphology of the  
713 Wadati-Benioff zone and seismotectonic pattern of the continental wedge. *J. Southeast Asian Earth Sci.*, 13:  
714 39-60.

715 Ingersoll, R. V., 2012. *Tectonics of Sedimentary Basins: Recent Advances, First Edition*. Edited by Cathy Busby and  
716 Antonio Azor Perez. 2012 Blackwell Publishing Ltd.

717 Jarrard, R.D., 1986. Terrane motion by strike-slip faulting of fore-arc slivers. *Geology*, 14, 780–783.

718 Kim, Y.-S., Peacock D. C.P., Sanderson D. J., 2004. Fault damage zones. *Journal of Structural Geology*, 26, 503–517.

719 Knott, S. D., 1987. The Liguride Complex of Southern Italy: A Cretaceous to Paleogene accretionary wedge:  
720 *Tectonophysics*, v. 142, pp. 217-226

721 Knott S. D., Turco E., 1991. Late Cenozoic kinematics of the Calabrian Arc, southern Italy. *Tectonics*, 10: pp. 1164-  
722 1172.

723 Langone, A., Gueguen, E., Prosser G., Caggianelli A., Rottura, A., 2006. The Curinga - Girifalco fault zone (northern  
724 Serre, Calabria) and its significance within the Alpine tectonic evolution of the western Mediterranean. *Journal*  
725 *of Geodynamics*, 42, pp. 140 - 158.

726 Li, H., Michelini, A., Zhu, L., Bernardi, F., Spada, M. 2007 - Crustal velocity structure in Italy from analysis of regional  
727 seismic waveforms. *Bulletin of the Seismological Society of America* 97, pp. 2024–2039.  
728 <http://dx.doi.org/10.1785/0120070071>.

729 Liberi, F., Morten, L., Piluso, E. 2006. Geodynamic significance of ophiolites within the Calabrian Arc. *Island Arc* 15,  
730 pp. 26–43.

731 Longhitano, S. G., Chiarella, D., Muto F., 2014. Three-dimensional to two-dimensional cross-strata transition in the  
732 lower Pleistocene Catanzaro tidal strait transgressive succession (southern Italy), *Sedimentology*. 61, 2136–  
733 2171 doi: 10.1111/sed.12138.

734 Longhitano, S.G., Chiarella, D., Di Stefano, A., Messina, C., Sabato, L., Tropeano, M., 2012b. Tidal signatures in  
735 Neogene to Quaternary mixed deposits of southern Italy straits and bays. In: *Modern and Ancient Depositional*  
736 *Systems: Perspectives, Models and Signatures* (Eds S.G. Longhitano, D. Mellere and R.B. Ainsworth), *Sed.*  
737 *Geol. Spec. Issue*, 279, 74–96.

738 Loreto, M.F., Fracassi, U., Franzo, A., Del Negro P., Zgur F., Facchin L., 2013. Approaching the potential seismogenic  
739 source of the 8 September 1905 earthquake: New geophysical, geological and biochemical data from the S.  
740 Eufemia Gulf (S Italy). *Marine Geology*, 343, pp. 62–75.

741 Loreto, M.F., Zgur F., Facchin L., Fracassi U., Pettenati F., Tomini I., Burca M., Diviacco P., Sauli C., Cossarini G., De  
742 Vittor C., Sandron D., the Explora technicians team, 2012. In *Search of New Imaging For Historical*  
743 *Earthquakes: A New Geophysical Survey Offshore Western Calabria (Southern Tyrrhenian Sea, Italy)*, *Boll.*  
744 *Geof. Teor. App.*, v. 53. <http://dx.doi.org/10.4430/bgta0046>.

745 Maffione M., Speranza F., Cascella A., Longhitano S. G., Chiarella D., 2013. A ~125° post-early Serravallian  
746 counterclockwise rotation of the Gorgoglione Formation (Southern Apennines, Italy): New constraints for the  
747 formation of the Calabrian Arc. *Tectonophysics* Vol. 590, pp 24–37.

748 Malinverno, A., Ryan, W.B.F., 1986. Extension in the tyrrhenian sea and shortening in the apennines as result of arc  
749 migration driven by sinking of the lithosphere. *Tectonics* 5, 227–245.

750 Mantovani, E., Babbucci, D., AlbareIlo, D., Mucciarelli, M., 1990. Deformation pattern in the central Mediterranean  
751 and behavior of the Africa/Adriatic promontory. *Tectonophysics*, 179: 63-79.

752 Manzi, V., Lugli, S., Roveri, M., Schreiber, B.C., Gennari, R., 2010. The Messinian “Calcare di Base” (Sicily, Italy)  
753 revisited. *Geologica Society of America Bulletin*. doi:10.1130/B30262.1.

754 Mattei M., Cifelli F., D’Agostino N., 2007. The evolution of the Calabrian arc: Evidence from paleomagnetic and GPS  
755 observations, *Earth Planet. Sci. Lett.*, 263, pp. 259-274.

756 Mattei, M., Argentieri, A., Rossetti, F., Speranza, F., Sagnotti, L., Funicello, R., 1999. Extensional tectonic in the  
757 Amantea Basin: a comparison between AMS and structural data. *Tectonophysics* 307, pp. 33-49.

758 Messina, A., Russo, S., Borghi, A., Colonna, V., Compagnoni, R., Caggianelli, A., Fornelli, A., Piccarreta, G., 1994. Il  
759 Massiccio della Sila, Settore settentrionale dell’Arco Calabro-Peloritano (The Sila Massif, northern sector of  
760 the Calabrian-Peloritan Arc). *Bollettino della Societ`a Geologica Italiana* 113, pp. 539–586.

761 Messina, A., Compagnoni, R., De Vivo, B., Perrone, V., Russo, S., Barberi, M., Scott, B., 1991a. Geological and  
762 petrochemical study of the Sila Massif plutonic rocks (Northern Calabria, Italy). *Boll. Soc. Geol. It.*, **110**, 165-  
763 206.

764 Messina, A., Russo, S., Perrone, V., Giacobbe, A., 1991b. Calcalkaline Late Variscan two micacordierite-Al silicate-  
765 bearing intrusion of the Sila batholith (northern sector of the Calabrian- Peloritan Arc, Italy). *Boll. Soc. Geol.*  
766 *It.*, 110, pp. 365-389.

767 Miyauchi, T., Dai Pra, G., Labini, S.S., 1994. Geochronology of Pleistocene marine terraces and regional tectonics in  
768 the Tyrrhenian coast of South Calabria, Italy. *Il Quaternario* 7, 17–34.

769 Milia A., Turco E., Pierantoni P.P., Schettino A., 2009. Four-dimensional tectonostratigraphic evolution of the Southern  
770 peri-Tyrrhenian Basins (Margin of Calabria, Italy). *Tectonophysics* 476, pp. 41–56.

771 **Minelli L., Faccenna C., 2010. Evolution of the Calabrian accretionary wedge (central Mediterranean). *Tectonics* 29:**  
772 **TC4004. doi: 10.1029/2009TC002562**

773 Monaco, C., Tortorici, L., 2000. Active faulting in the Calabrian Arc and eastern Sicily. *Journal of Geodynamics*, 29,  
774 pp. 407–424.

775 Monaco, C., Tortorici, L., Nicolich, R., Cernobori, L., Costa, M., 1996. From collisional to rifted basins: an example  
776 from the southern Calabrian Arc (Italy). *Tectonophysics* 266, pp. 233–249.

777 Muto F., Perri E., 2002. Evoluzione tettono - sedimentaria del bacino di Amantea, Calabria occidentale. *Boll. Soc. Geol.*  
778 *It.*, 121, pp. 391 - 409.

779 **Muto, F., Spina, V., Tripodi, V., Critelli, S., Roda, C., 2014. Neogene tectonostratigraphic evolution of allochthonous**  
780 **terrane in the eastern Calabrian foreland (southern Italy). *Ital. J. Geosci.* 133, 455–473.**

781 Neri G, Barberi G, Oliva G, Orecchio B., 2004. Tectonic stress and seismogenic faulting in the area of the 1908  
782 Messina earthquake, south Italy. *Geophys Res Lett* 31:10. doi:10.1029/2004 GL019742

783 Neri G., Orecchio B., Totaro C., Falcone G., Presti D., 2009. Subduction beneath southern Italy close the ending: results  
784 from seismic tomography. *Seismol. Res. Lett.*, 80, pp. 63-70.

785 Neri, G., Caccamo, D., Cocina, O., Montalto, A., 1996. Geodynamic implications of earthquake data in the southern  
786 Tyrrhenian sea. *Tectonophysics* 258, pp. 233–249.

787 Ogniben, L., 1973. Schema geologico della Calabria in base ai dati odierni. *Geologica Romana*, 12, pp. 243-585.

788 Ogniben, L., 1969. Schema introduttivo alla geologia del confine calabro-lucano (Introductory scheme to the geology of  
789 the Calabrian-Lucanian boundary). *Memorie della Societ`a Geologica Italiana* 8, 453–763.

790 Peacock D.C.P., Parfitt E.A., 2002. active relay ramps and fault propagation on Kilauea Volcano, Hawaii. *Journal of*  
791 *Structural Geology*, 24, pp. 729-744.

792 Peacock, D.C.P., Knipe, R.J., Sanderson, D.J., 2000. Glossary of normal faults: *Journal of Structural Geology*, v. 22, p.  
793 291–306.

794 Pepe, F., Sulli, A., Bertotti, G., Cella, F., 2010. Architecture and Neogene to recent evolution of the western Calabrian  
795 continental margin: an upper plate perspective to the Ionian subduction system, central Mediterranean.  
796 *Tectonics* 29, TC3007. [Doi.org/10.1029/2009TC002599](https://doi.org/10.1029/2009TC002599).

797 Presti, D., Billi, A., Orecchio, B., Totaro, C., Faccenna, C., Neri, G., 2013. Earthquake focal mechanisms, seismogenic  
798 stress, and seismotectonics of the Calabrian Arc, Italy, *Tectonophysics*. [doi.org/10.1016/j.tecto.2013.01.030](https://doi.org/10.1016/j.tecto.2013.01.030)

799 Roda, C., 1964. Distribuzione e facies dei sedimenti neogenici nel Bacino Crotonese. *Geol. Rom.*, 3: 319-366.

800 Roveri, M., Lugli, S., Manzi, V., Schreiber, B.C., 2008. The Messinian salinity crisis: a sequence- stratigraphic  
801 approach. *GeoActa*, Special Publication, 1, pp. 117-138.

802 Rovida, A., Camassi, R., Gasperini, P., Stucchi, M., 2011. CPTI11, the 2011 version of the Parametric Catalogue of  
803 Italian Earthquakes. Milano, Bologna. <http://emidius.mi.ingv.it/CPTI>.

804 Salvini, F., 2002. The Structural Data Integrated System Analyzer. Version 3.43b (11/12/2002). Dept. of Earth  
805 Sciences, University “Roma Tre”, Rome, Italy, Free software available upon request at:  
806 <http://www.dea.uniroma3.it/begin.htm>.

807 Salvini, F., Vittori, E., 1982. Analisi strutturale della linea Olevano-Antròdoco-Posta (Ancona-Anzio Auct.):  
808 metodologia di studio delle deformazioni fragili e presentazione del tratto meridionale. *Mem. Soc. Geol. Ital.*  
809 24, pp. 337-356.

810 Serpelloni, E., Vannucci, G., Pondrelli, S., Argnani, A., Casula, G., Anzidei, M., Baldi, P., Gasperini, P., 2007.  
811 Kinematics of the western Africa–Eurasia plate boundary from local machanisms and GPS data. *Geophysical*  
812 *Journal International* 169, pp. 1180–1200.

813 Serpelloni, E., R. Bürgmann, M. Anzidei, P. Baldi, Mastrolembo Ventura B., Boschi E., 2010. Strain accumulation  
814 across the Messina Straits and kinematics of Sicily and Calabria from GPS data and dislocation modeling,  
815 Earth Planet. Sc. Lett., 298(3–4), pp. 347–360..

816 Sieh, K., Natawidjaja, D., 2000. Neotectonics of the Sumatran fault, Indonesia. *Journal of Geophysical Research*, 105,  
817 pp. 28 295–28 326.

818 Sylvester, A. G., 1988. Strike-slip faults. *Geological Society of America Bulletin*, 100, pp. 1666–1703.

819 Tansi, C., Muto, F., Critelli S., Iovine G., 2007. Neogene–Quaternary strike-slip tectonics in the central Calabria Arc  
820 (southern Italy). *J. Geodyn.*, 43, pp. 397–414.

821 Tortorici, G., Bianca, M., De Guidi, G., Monaco, C., Tortorici, L., 2003. Fault activity and marine terracing in the Capo  
822 Vaticano area (southern Calabria) during the Middle-Late Quaternary, *Quat. Int.*, 101-102, 269-278.

823 Tortorici, G., Bianca, M., Monaco, M., Tortorici, L., Tansi, C., De Guidi, G., Catalano S., 2002. Quaternary normal  
824 faulting and marine terracing in the area of Capo Vaticano and S. Eufemia Plain (Southern Calabria, Italy).  
825 *Studi Geologici Camerti*, 2, pp. 1 - 16.

826 Tortorici, L., Monaco, C., Tansi, C., Cocina, O., 1995. Recent and active tectonics in the Calabrian arc (Southern Italy).  
827 *Tectonophysics* 243, 37–55.

828 Tortorici, L., 1982. Lineamenti geologico-strutturali dell'Arco Calabro Peloritano (Geologic-structural lineaments of  
829 the Calabrian-Peloritan Arc). *Società Italiana di Mineralogia e Petrografia* 38, 927–940.

830 Trincardi, F. Cipolli, M., Ferretti, P., La Morgia, J., Ligi, M., Marozzi, G., Palumbo, V., Taviani, M., Zitellini N., 1987.  
831 Slope basin evolution on the Eastern Tyrrhenian margin: preliminary report. *Giornale di Geologia*, ser. 3", vol.  
832 49/2, pp. 1-9.

833 Tripodi, V., Muto, F., Critelli, S., 2013. Structural style and tectono-stratigraphic evolution of the Neogene- Quaternary  
834 Siderno Basin, southern Calabrian Arc, Italy. *Int. Geol. Rev.*, 4, pp. 468–481.

835 Turco, E., Maresca, R., Cappadona, P., 1990. La tettonica plio-pleistocenica del confine calabro-lucano: modello  
836 cinematico (Plio-Pleistocene tectonics at the Calabrian-Lucanian boundary: a kinematic model). *Memorie della*  
837 *Società Geologica Italiana*, 45, pp. 519–529.

838 Van Dijk, J.P., Bello, M., Brancaleoni, G.P., Cantarella, G., Costa, V., Frixia, A., Golfetto, F., Merlini, S., Riva, M.,  
839 Torricelli, S., Toscano, C., Zerilli, A., 2000. A regional structural model for the northern sector of the  
840 Calabrian Arc (southern Italy). *Tectonophysics*, 324, pp. 267-320.

841 Van Dijk, J.P., Scheepers, P.J.J., 1995. Neogene rotations in the Calabrian Arc. Implications for a Pliocene–Recent  
842 geodynamic scenario for the Central Mediterranean. *Earth Sci.* 241–270. *Rev.* 39, 207–246.

- 843 Vezzani, L., 1967. Il bacino plio-pleistocenico di S. Arcangelo (Lucania). *Atti Accad. gioenia sci. nat. Catania* 18, 207–  
844 227.
- 845 Waldrom, J.W.F., 2005. Extensional fault arrays in strike-slip and transtension. *Journal of Structural Geology* 27, pp.  
846 23–34
- 847 Westaway R., 1993: Quaternary uplift of Southern Italy. *Journal of Geophysical Research* 98 (B12), pp. 741–772.
- 848 Wise D.U., Vincent R.J. 1965. Rotation axis method for detecting conjugate planes in calcite petro-fabric. *American*  
849 *Journal of Science*. 263, pp. 289-301.
- 850 Wortel, R., Spakman W., 2000. Subduction and slab detachment in the Mediterranean-Carpathian region. *Science*, 290,  
851 pp. 1910-1917.
- 852 Wortel, M.J.R., Spakman, W., 1992. Structure and dynamics of subducted lithosphere in the Mediterranean  
853 region; *Proceedings of the Koninklijke Nederlandse Akademie Van Wetenschappen-Biological Chemical*  
854 *Geological Physical and Medical Sciences*, 95, pp. 325–347.
- 855 Zecchin, M., Caffau, M., Civile, D., Critelli, S., Di Stefano, A., Maniscalco, R., Muto, F., Sturiale, G., Roda, C., 2012.  
856 The Plio-Pleistocene evolution of the Croton Basin (southern Italy): interplay between sedimentation,  
857 tectonics and eustasy in the frame of Calabrian Arc migration. *Earth-Sci. Rev.*, 115, pp. 273-303.
- 858 Zecchin, M., Caffau, M., Di Stefano, A., Maniscalco, R., Lenaz, D., Civile, D., Muto, F., Critelli, S., 2013a.  
859 The Messinian succession of the Croton Basin (southern Italy) II: Facies architecture and stratal surfaces  
860 across the Miocene–Pliocene boundary. *Mar. Pet. Geol.* 48, 474–492.
- 861 Zecchin, M., Civile, D., Caffau, M., Muto, F., Di Stefano, A., Maniscalco, R., Critelli, S., 2013b. The Messinian  
862 succession of the Croton Basin (southern Italy) I: Stratigraphic architecture reconstructed by seismic and well  
863 data. *Mar. Pet. Geol.* 48, 455–473.
- 864 Zecchin, M., Praeg, D., Ceramicola, S., Muto, F., 2015. Onshore to offshore correlation of regional unconformities in  
865 the Plio-Pleistocene sedimentary successions of the Calabrian Arc (central Mediterranean). *Earth- Science*  
866 *Reviews* 142, pp. 60–78.